UNIVERSIDADE DA BEIRA INTERIOR
Ciências da Saúde

Impact of H-ferritin deficiency on macrophage viability and iron status

Gonçalo Augusto Taborda da Costa Laranja Mesquita

Dissertação para obtenção do Grau de Mestre em
Ciências Biomédicas
(2º ciclo de estudos)
(Tese definitiva após defesa pública)

Orientador: Doutora Ana Carolina Moreira
Co-orientador: Prof. Doutora Maria Salomé Gomes
Co-orientador: Prof. Doutor Fernando A. Arosa

Covilhã, Outubro de 2017

Dedicatória

Esta tese é dedicada:

- À minha avó, que me apoia todos os dias e que me faz acreditar sempre, que sou capaz de ultrapassar todos os desafios que me apareçam;
- À Tânia Silva, que, mesmo sem ter essa responsabilidade, me apoiou em todos os aspetos no desenvolvimento desta tese;
- Aos meus irmãos.

Agradecimentos

Para começar queria agradecer aos meus orientadores da tese, à Doutora Carolina Moreira, à Professora Doutora Salomé Gomes e ao Professor Doutor Fernando Arosa. Um agradecimento especial à Carolina que, mais do que orientadora, é uma das pessoas mais espantosas que conheço e que se tornou numa boa amiga. Também um agradecimento especial à Professora Salomé que nunca deixou de acreditar em mim, mesmo com os percalços que fui tendo ao longo desta jornada. Quero agradecer à Universidade da Beira Interior à qual pertenci durante 5 anos e da qual vou levar imensas experiências e pessoas que ficarão comigo durante o resto da minha vida. Um agradecimento, também, ao i3S por me permitir realizar a tese nas suas instalações, não podendo esquecer um agradecimento ao Professor Doutor Pedro Rodrigues por me acolher no seu grupo, Iron and Innate Immunity. Neste grupo tenho de agradecer à Carolina (mais nova), ao João, à Tânia, a quem já dediquei esta tese e à Rita, que sempre se mostrou disponível para me ensinar e ajudar em tudo. Obrigado por tornarem o dia-a-dia no laboratório num ambiente sempre alegre e familiar. Para isto também ajudou muito a companhia do pessoal do grupo Immune Regulation a quem também deixo uma nota de apreço. Agradecer também ao ICBAS, por me permitir usar as suas instalações para o desenvolvimento desta tese.

Na parte mais pessoal, quero deixar um muito obrigado à minha família. Em especial, para os meus pais, pela educação que me deram e pelos sacrifícios que tiverem de fazer para eu chegar onde cheguei, não tenho palavras para descrever o quão grato estou. Gostava de poder expressar individualmente a minha gratidão pela minha segunda família, que são os meus amigos. No entanto isso ocuparia demasiado espaço e iria deixar demasiados egos inchados. No entanto, aos meus amigos, sejam eles de Famalicão, Covilhã ou de outra cidade qualquer, obrigado por me aturarem e não me deixarem ir abaixo mesmo em momentos menos bons. Em especial, àqueles que convivem comigo todos os dias, esta tese é um bocadinho de cada um de vocês. A quem não referi e que participou, direta ou indiretamente, nesta tese, deixo aqui a minha nota de agradecimento.

Este trabalho foi financiado pelos fundos da FEDER - Fundo Europeu de Desenvolvimento Regional, através do COMPETE2020 – Programa Operacional para a Competitividade e Internacionalização (POCI), Portugal 2020 e por fundos portugueses, através da FCT - Fundação para a Ciência e a Tecnologia/Ministério da Ciência, Tecnologia e Ensino Superior, no âmbito do projeto PTDC/IMI-MIC/1683/2014 (POCI-01-0145-FEDER-016590).

FCT
Fundação para a Ciência e a Tecnologia
MINISTÉRIO DA CIÊNCIA, TECNOLOGIA E ENSINO SUPERIOR

Cofinanciado por:

COMPETE 2020 PORTUGAL 2020 UNIÃO EUROPEIA
Fundo Europeu
de Desenvolvimento Regional

Resumo

O ferro é essencial para a sobrevivência de quase todos os organismos vivos, sendo um elemento fundamental em diversas funções celulares, como a síntese do ADN e do ARN, proliferação celular e produção de energia. No entanto, este mineral necessita de ser cuidadosamente regulado e armazenado. Para tal, o metabolismo do ferro necessita de ser controlado a nível sistémico e celular. O ferro que não se encontra armazenado, ou ligado a alguma proteína, pode participar em reações que levam à formação de radicais livres, que podem promover a degradação o ADN, ARN, proteínas, entre outros. Para evitar estes efeitos nefastos, as células desenvolveram vários mecanismos, entre eles, a ferritina. A ferritina é uma proteína composta por duas subunidades, a H e a L, que são responsáveis pelo armazenamento do ferro.

Os macrófagos têm um papel essencial, tanto na resposta imune à infeção, como no metabolismo e distribuição do ferro. Estudos anteriores do nosso laboratório demonstraram que quando infetados com micobactérias os macrófagos aumentam os seus níveis de ferritina-H (FTH1). O objetivo desta tese foi investigar o papel da FTH1 na biologia do macrófago. Para tal, foram usados macrófagos derivados da medula óssea de murganhos, com uma deleção condicional da ferritina-H, na linhagem mieloide. Os nossos resultados começaram por demonstrar que a FTH1 não é necessária à diferenciação dos macrófagos, a partir dos seus precursores. Além disso, a viabilidade e a expressão de genes relacionados com o metabolismo do ferro também não foram diferentes em macrófagos deficientes em FTH1. No entanto, quando estimulados por ferro exógeno, a viabilidade celular destes macrófagos diminuiu e, de forma concordante, a morte celular aumentou. Estes fenómenos, podem estar a ocorrer devido a um aumento do ferro livre e subsequente aumento de dano devido ao stress oxidativo.

Posteriormente, analisámos o impacto da FTH1 na resposta dos macrófagos a estímulos imunológicos e/ou bacterianos. Pudemos concluir que há um claro papel da FTH1 na proteção contra a toxicidade do IFN-γ, sendo que os macrófagos que não expressavam *Fth1*, tiveram a sua viabilidade reduzida e uma maior percentagem de morte celular. A expressão génica, de outros elementos envolvidos no metabolismo do ferro, nos macrófagos desprovidos de *Fth1*, também se encontrava alterada, com especial foco em células tratadas com IFN-γ+LPS. Além disso, a produção de nitritos nestas células encontrava-se diminuída.

Em conclusão, estes resultados indicam um papel preponderante da FTH1 na proteção celular contra a toxicidade induzida tanto pelo ferro, como pelo IFN-γ. Num trabalho futuro, pretendemos aprofundar os mecanismos responsáveis pela proteção conferida pela FTH1, aos macrófagos, assim como abordar o seu papel num contexto de infeção.

Palavras-chave

Ferritina-H; macrófagos derivados de medula óssea; metabolismo do ferro.

Abstract

Almost all life on Earth has a great demand for iron. Importance of iron is based on its crucial participation on several fundamental processes such as DNA and RNA synthesis, cell proliferation and energy production. However, this mineral needs to be strictly controlled and properly stored, as free iron can induce tissue and cell damage through the formation of free radicals. Iron traffic and distribution is controlled by complex systems, operating both at systemic and at cellular levels. Ferritin plays a key role in this respect. The ferritin protein, composed of H and L subunits, is responsible for safely storing iron inside the cells. Macrophages are central cells both for immune response to infection and for the iron metabolism and distribution. Previous work of our group showed that macrophages infected with mycobacteria increase their content in H-ferritin (FTH1).

The main goal of this thesis was to investigate the role of FTH1 in macrophage physiology, using bone marrow-derived macrophages from mice with a conditional deletion of *Fth1* in the myeloid lineage. Our data showed that FTH1 was not necessary for macrophages' differentiation from bone marrow precursors. FTH1-deficient macrophages kept their viability and had a normal expression of iron-related genes. Nonetheless, when challenged with exogenous iron, macrophages lacking *Fth1* have increased mortality, probably due to the increase in free iron and subsequent increase in oxidative damage.

Furthermore, the impact of *Fth1* on macrophage response to both immune and bacterial stimuli was studied. Our results demonstrated a clear role for H-ferritin in protection against IFN-γ toxicity, as cells that do not express *Fth1* had their viability impaired alongside with higher mortality. Gene expression of iron metabolism-related genes, between genotypes, was altered, especially in cells treated with IFN-γ+LPS. Additionally, nitrites production was hampered in macrophages lacking *Fth1*.

In conclusion, these findings indicate that FTH1 is essential for cellular protection against iron and IFN-γ-induced toxicity. Future work will deepen our knowledge onto the mechanisms behind the protective role of FTH1 in macrophages, against these different external insults, and also in the context of infection.

Keywords

H-ferritin; bone marrow-derived macrophages; iron metabolism.

Resumo Alargado

O ferro é essencial para a sobrevivência de quase todos os organismos vivos, sendo fundamental em diversas funções celulares, como a síntese do ADN e do ARN, proliferação celular e produção de energia. No entanto, este mineral necessita de ser cuidadosamente regulado e armazenado, de forma a não ser prejudicial para os tecidos e células. Para tal, o metabolismo do ferro necessita de ser controlado a nível sistémico e celular. O ferro que não se encontra armazenado, ou ligado a alguma proteína, pode participar em reações que levam à formação de radicais livres, que podem promover a degradação do ADN, ARN, proteínas, entre outros. Para evitar estes efeitos nefastos, as células desenvolveram vários mecanismos, entre eles, a ferritina. A ferritina é uma proteína composta por duas subunidades, a H e a L, que são responsáveis pelo armazenamento do ferro.

Os macrófagos têm um papel essencial, tanto na resposta imune à infeção, como no metabolismo e distribuição do ferro. Estudos anteriores do nosso laboratório, demonstraram que quando infetados com micobactérias os macrófagos aumentam os seus níveis de ferritina-H (FTH1). O objetivo do trabalho desta tese, foi investigar o papel da FTH1 na biologia do macrófago. Para tal, foram usados macrófagos derivados da medula óssea de murganhos, com uma deleção condicional da ferritina-H, na linhagem mieloide. Os nossos resultados começaram por demonstrar que, efetivamente, tanto a nível génico, como a nível proteico, confirmou-se a deleção da ferritina-H. De seguida, analisamos o desenvolvimento dos macrófagos que não possuíam ferritina-H, de forma a perceber se esta tinha algum impacto na sua diferenciação a partir dos precursores. Para tal, recorremos a testes de viabilidade, citometria de fluxo e microscopia. Estes resultados demonstraram que a FTH1 não tem um papel essencial no desenvolvimento e diferenciação dos macrófagos. O passo seguinte, foi a análise da expressão de genes envolvidos no metabolismo do ferro e de genes relativos à ativação macrofágica, na qual não foram observadas diferenças significativas entre os genótipos.

Uma vez que não se registaram diferenças em condições basais, decidimos estimular as células com diferentes compostos exógenos. Os primeiros estímulos testados foram duas diferentes fórmulas de ferro, FAC e hemina, e um quelante, denominado DFO. Ambas as formas de ferro foram tóxicas para as células. Através da análise da viabilidade e morte celular, na presença de concentrações crescentes das duas formas de ferro, foi calculado o IC_{50}, a concentração necessária para um composto reduzir a viabilidade celular em 50%, para cada uma delas. Verificámos deste modo que as células foram mais suscetíveis (IC50 mais baixo) ao FAC do que à hemina e que os macrófagos deficientes em *Fth1* eram mais suscetíveis a ambas as formas de ferro do que os macrófagos normais. O quelante DFO não induziu efeitos diferentes entre os dois genótipos e não conseguiu reduzir a viabilidade celular abaixo dos 50%, pelo que não foi possível calcular IC_{50} para este composto.

Por último, averiguamos o papel da ferritina-H na ativação dos macrófagos. Com este objetivo, incubámos macrófagos, que possuem, ou não, a deleção condicional do gene da ferritina-H, com dois conhecidos ativadores macrofágicos, IFN-γ e LPS. Nesta parte do trabalho, analisámos a viabilidade, morte celular, expressão génica e produção de nitritos e TNF-α dos macrófagos. Nos vários testes realizados, encontraram-se algumas diferenças nas respostas dos dois genótipos. Macrófagos desprovidos de *Fth1* são mais suscetíveis ao IFN-γ e na presença de IFN-γ+LPS expressam menos *Tfrc* (gene do recetor da transferrina-1) e *Nos2a* (gene do indutor da síntese de óxido nítrico), além de terem uma menor produção de nitritos.

Em conclusão, estes resultados demonstram que a FTH1 não é preponderante para o desenvolvimento e diferenciação dos macrófagos, mas tem um papel na resposta a estímulos exógenos. As experiências realizadas indicam um papel preponderante da FTH1 na proteção celular contra a toxicidade induzida tanto pelo ferro, como pelo IFN-γ. Num trabalho futuro, pretendemos aprofundar os mecanismos responsáveis na proteção conferida pela FTH1, aos macrófagos, assim como abordar o seu papel num contexto de infeção.

Palavras-chave

Ferritina-H; macrófagos derivados de medula óssea; metabolismo do ferro.

Contents

Figures' list

Figure 6 – Mo-*Fth1*$^{-/-}$ and Mo-*Fth1*$^{+/+}$ have similar morphologies. Light microscopy images of BMM at **A)** 8 and **B)** 10 days after the beginning of the culture. Pictures shown here are representative of four independent experiments. The cells were visualized and photographed in an Olympus SC30 camera.

Figure 7 – Mo-*Fth1*$^{-/-}$ do not express H-Ferritin. A) 10 days after the beginning of the culture, BMM were harvested, total protein quantified and H-ferritin (FTH1) expression was determined by Western blot. ß-actin (ACTB) was used as housekeeping protein (loading control). These results are representative of two independent experiments. **B)** The graph represents the densitometry analysis obtained with ImageLab™ software of FTH1 expression in each culture, normalized to ACTB densitometry, expressed as percentage to Mo-*Fth1*$^{+/+}$. Statistical analysis was performed using an unpaired t test. * $p < 0.05$ statistically significant.

Figure 8 – **Expression of iron metabolism genes are similar in both genotypes.** 10 days after the beginning of the culture, qPCR was used to determine the expression levels of several genes involved in iron metabolism: H-ferritin *(Fth1)*, L-ferritin (*Ftl*), ferroportin (*Slc40a1*), heme oxygenase 1 (*Hmox1*), transferrin receptor (*Tfrc*), inducible nitric oxide synthase *(Nos2a)*, arginase (*Arg1*) and tumor-necrosis factor (*Tnf*). Data represent the mean + SD are expressed as the fold-change of expression in Mo-*Fth1*$^{-/-}$ (grey bars) relative to that in Mo-*Fth1*$^{+/+}$ (dashed line). Number of samples for each gene is depicted in the graph. Statistical analysis was performed using unpaired t-test. * $p < 0.05$ statistically significant.

Figure 9 – Mo-*Fth1*$^{-/-}$ are more sensitive to iron toxicity. Mo-*Fth1*$^{+/+}$ (black) and Mo-*Fth1*$^{-/-}$ (grey) were treated with FAC (**A**), hemin (**B**) or the iron chelator DFO (**C**) at different concentrations, 7 days after the beginning of the culture. Cell viability was measured 3 days later, by resazurin reduction: resazurin (0.3 mg/ml) was added at 10% (v/v), incubated for 20 h, and the fluorescence was measured at 530/590 nm. The graphs represent the mean ± SD (n[Mo-*Fth1*$^{+/+}$] = 3; n[Mo-*Fth1*$^{-/-}$] = 7). Statistical analysis was performed using two-way ANOVA with Tukey's multiple comparisons. * $p < 0.05$ statistically significant.

Figure 10 – Cell viability of Mo-*Fth1*$^{-/-}$ decreases in the presence of iron. Mo-*Fth1*$^{+/+}$ (black) and Mo-*Fth1*$^{-/-}$ (grey) were treated with FAC (**A**), hemin (**B**) or the iron chelator DFO (**C**) at different concentrations, 7 days after the beginning of the culture. Cell death was measured through SYTOX™ Green three days after the treatment. The graphs represent the mean + SD (n[Mo-*Fth1*$^{+/+}$] = 2; n[Mo-*Fth1*$^{-/-}$] = 4). Statistical analysis was performed using two-way ANOVA with Tukey's multiple comparisons. * $p < 0.05$ statistically significant. (**D**) Cell death was analyzed through TUNEL assay. Mo-*Fth1*$^{+/+}$ (black) and Mo-*Fth1*$^{-/-}$ (grey) were treated with 30 µM FAC, 100 µM hemin and 100 µM DFO, for 72 h. The graph represents one experiment (n[Mo-*Fth1*$^{+/+}$] = 1; n[Mo-*Fth1*$^{-/-}$] = 1).

Figure 11 - Mo-*Fth1*$^{-/-}$ have an increased susceptibility to IFN-γ. Cells were treated with IFN-γ, LPS or IFN-γ+LPS, 7 days after the beginning of the cell culture. Cell viability (A) and cell

death (B) Mo-*Fth1*$^{+/+}$ (black) and Mo-*Fth1*$^{-/-}$ (grey) were measured 3 days after treatments. A) Resazurin (0.3 mg/ml) was added at 10% (v/v), incubated for 20 h, and fluorescence was measured at 530/590 nm. The graph represents the mean + SD of five independent experiments (n[Mo-*Fth1*$^{+/+}$] = 3; n[Mo-*Fth1*$^{-/-}$] = 7). B) Cell death was measured through SYTOX™ Green. The graph represents the mean + SD (n[Mo-*Fth1*$^{+/+}$] = 2; n[Mo-*Fth1*$^{-/-}$] = 4). * $p < 0.05$ when comparing the two genotypes. # $p < 0.05$ statistically significant when comparing with the corresponding NT sample.

Figure 12 – **Iron metabolism genes have different expression responses to cytokines in Mo-*Fth1*$^{+/+}$ and Mo-*Fth1*$^{-/-}$.** After 7 days in culture, BMM were treated with IFN-γ, LPS or IFN-γ+LPS, and 3 days later the expression levels of several iron metabolism genes were quantified by qPCR. (**A**) H-ferritin (*Fth1*), (**B**) L-ferritin (*Ftl*), (**C**) ferroportin (*Slc40a1*), (**D**) heme oxygenase 1 (*Hmox1*), (**E**) transferrin receptor (*Tfrc*) and (**F**) inducible nitric oxide synthase (*Nos2a*). Data are expressed as mean + SD, presented as fold-change relatively to the non-treated (NT) Mo-*Fth1*$^{+/+}$ (n[Mo-*Fth1*$^{+/+}$] = 4; n[Mo-*Fth1*$^{-/-}$] = 7). Statistical analysis was performed using two-way ANOVA with Tukey's multiple comparisons. * $p < 0.05$ statistically significant between the two genotypes; # $p < 0.05$ statistically significant when comparing with the NT of Mo-*Fth1*$^{+/+}$.

Figure 13 – Nitrite production is altered in Mo-*Fth1-/-*. Cells were treated with IFN-γ, LPS or IFN-γ+LPS, 7 days after the beginning of the cell culture. Nitrite production (**A**) and release of TNF-α (**B**) of Mo-*Fth1*$^{+/+}$ (black) and Mo-*Fth1*$^{-/-}$ (grey) was measured 3 days after cytokines treatment. **A**) Nitrite production was quantified by the Griess assay. **B**) TNF-α production was measured by ELISA. The graphs represent the mean + SD (n[Mo-*Fth1*$^{+/+}$] = 2; n[Mo-*Fth1*$^{-/-}$] = 6). Statistical analysis was performed using two-way ANOVA with Tukey's multiple comparisons test. * $p < 0.05$ when comparing the two genotypes. # $p < 0.05$ statistically significant when comparing with the corresponding NT sample.

Tables' List

Abbreviation List

ACTB [a] - ß-actin

Arg1 [a] – Arginase gene

BM - Bone marrow

BMM – Bone marrow-derived macrophages

BSA – Bovine serum albumin

CT – Threshold cycle

CYBRD1 - Cytochrome b reductase 1

DFO – Desferoxamine B mesylate

DMEM – Dulbecco's modified eagle medium

DMT1 - Divalent metal transporter-1

EP - Erythroid precursors

FAC – Ferric ammonium citrate

FBS – Fetal bovine serum

FSC – Forward scatter

Fth1 or FTH1[a] – H-ferritin gene or protein

Ftl or FTL[a] – L-Ferritin gene or protein

HBSS – Hank's salt balanced solution

Hmox1 or HMOX1[a] – Heme oxygenase 1 gene or protein

Hprt [a] – Hypoxanthine guanine phosphoribosyl transferase gene

HSC - Hematopoietic stem cells

IC_{50} – Half maximal inhibitory concentration

IFN-γ – Interferon-gamma

IRE - Iron responsive elements

IRP - Iron regulatory proteins

LCCM – L cell conditioned medium

LIP - Labile iron pool

LPS – Lipopolysaccharide

Lyz2 –Lysosome 2 gene

MAPK – mitogen-activated protein kinase

Mo-*Fth1*$^{-/-}$ - Macrophages deficient for *Fth1*

Mo-*Fth1*$^{+/+}$ - Macrophages sufficient for *Fth1*

NF-kB – nuclear factor kappa B

Nos2a or NOS2A[a] - Nitric oxide synthase gene or protein

NRAMP-1 – Natural resistance-associated macrophage protein-1

NT – Non-treated

PBS – Phosphate Buffered Saline

PFA - Paraformaldehyde

qPCR – Real-time PCR

[a] Accepted nomenclature by OMIM (www.omim.org) and Mouse Genomic Informatics (www.iformatics.jax.org).

RBC – Red blood cells

SD – Standard deviation

Slc40a1 or FPN1[a] - Ferroportin-1 gene or protein

SSC – Side scatter

STEAP3 - Six-transmembrane epithelial antigen of prostate 3

TBS-T – Tris-buffered saline with 0.1% Tween-20

TF – Transferrin

TFR2 - Transferrin-receptor 2

Tfrc or TFR1[a] - Transferrin receptor 1 gene or protein

TIM - T cell immunoglobulin-domain and mucin-domain

TLR –Tool-like receptor

Tnf or TNF-α[a] – Tumor necrosis factor gene or protein

TUNEL – Terminal deoxynucleotidyl transferase dUTP nick end labeling

 [a] Accepted nomenclature by OMIM (www.omim.org) and Mouse Genomic Informatics (www.iformatics.jax.org).

Chapter 1

Introduction

The Iron Metabolism

Regulation of iron absorption and distribution

Iron is essential for almost every living organism. It plays several key roles in diverse processes like synthesis of DNA or RNA, mitochondrial respiratory chain, cell proliferation and differentiation, among others (Lieu *et al.*, 2001). Specifically, in mammals, the most iron-demanding process is erythropoiesis. However, iron levels must be controlled, as either the lack or the excess of this metal can lead to serious health problems. Mammalian species have developed various mechanisms that can potentially protect them from the nefarious effects of both the lack and excess of iron. In case of iron deficiency, consequences can impact pregnancy (Allen, 2000), impair erythropoiesis and lead to anemia (Miller, 2013) or even affect the normal cognitive development (Jauregui-Lobera, 2014). When in excess or misplaced, iron may cause tissue and cell damage through formation of free radicals.

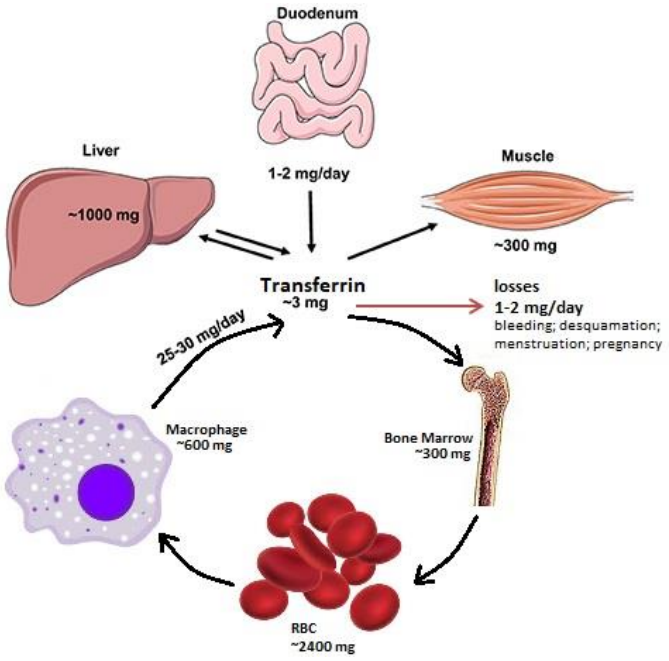

Figure 1 - Iron systemic cycle. Every day 1-2 mg of iron are absorbed through duodenum and transported into the bloodstream bound to transferrin. Iron can be stored in hepatocytes or used in the formation of new red blood cells (RBC). Iron inside erythrocytes can be recycled by macrophages and reused in the formation of new red blood cells. Iron losses occur through bleeding, desquamation, menstruation and pregnancy. Adapted from (Wilkinson and Pantopoulos, 2014).

The most well-known reactions that involve iron and can harm the cells are the "Haber-Weiss" and the "Fenton" reactions. In these, both ferrous iron (Fe^{2+}) and hydrogen peroxide interact with other substrates giving origin to radicals that are able to damage cell membranes, proteins and DNA (Eaton and Qian, 2002, Winterbourn, 1995). Iron toxicity can lead to several health problems, from cardiovascular diseases to cancer (Weinberg, 2009). In humans, iron represents approximately 45 mg/kg in male and female adults (Alleyne *et al.*, 2008). Iron values in the body do not vary much since there are almost no losses except for bleeding, pregnancy, menstruation or desquamation of epithelia (Nairz *et al.*, 2015) (Fig. 1). The small quantities of iron that enter the organism (1-2 mg a day) are absorbed through the duodenum and proximal jejunum, by the enterocytes. The extent of this absorption is tightly regulated by several factors. Ingested iron enters the enterocytes via the divalent metal transporter-1 (DMT1), located on the apical membrane of these cells. The most common form of iron in the diet is Fe^{3+}, however to be internalized by DMT1, iron needs to be in the ferrous form (Fe^{2+}). Thus, it is necessary to reduce it before it enters the enterocytes, which occurs mostly by cytochrome b reductase 1 (CYBRD1) (Latunde-Dada *et al.*, 2008). Heme-iron is also absorbed in the intestinal tract, but the mechanisms by which heme enters the enterocytes are not clear yet. After entering the cells, heme is degraded by heme oxygenase 1 (HMOX1) into carbon monoxide, free iron and bilirubin (Tenhunen *et al.*, 1968). Iron is exported from the cells by the only known iron exporter, ferroportin-1 (FPN1). This protein is essential in the iron homeostasis and when *Slc40a1*, ferroportin gene, is deleted it results in embryonic lethality (Donovan *et al.*, 2005). The levels of FPN1 at the cellular surface are controlled by hepcidin, a liver-produced hormone that induces the internalization and posterior degradation of the iron exporter (De Domenico *et al.*, 2009a, Nemeth *et al.*, 2004). Hepcidin expression is regulated by iron levels (Lin *et al.*, 2007), anemia (Wang and Babitt, 2016) and hypoxia (Liu *et al.*, 2012). When in conditions of iron overload, the levels of hepcidin increase leading to a decrease in FPN1 levels (D'Angelo, 2013). On the other hand, in situations of anemia or hypoxia there is a dramatic decrease in the hepcidin levels (Nicolas *et al.*, 2002). The link between iron levels and the expression of hepcidin in hepatocytes is regulated by bone morphogenic proteins and JAK2/STAT3 signaling pathway, hemojuvelin, neogenin, transferrin-receptor2 (TFR2), human hemochromatosis protein and BMP6 (reviewed in (Zhao *et al.*, 2013)).

The iron exported by FPN1 is oxidized by ferroxidases like hephaestin or ceruloplasmin, in order to be caught by the main iron transporter protein in the bloodstream, transferrin (TF) (Cherukuri *et al.*, 2005, Vulpe *et al.*, 1999). TF is an iron chelating protein that can bind two atoms of ferric iron (Fe^{3+}) in a reversible way, maintaining thus the iron in a tightly bound and low reactivity form, and preventing the generation of free radicals that could appear with the presence of ferrous iron (Fe^{2+}) (Aisen *et al.*, 1978).

Cell-intrinsic iron regulatory circuits

In order to internalize iron from transferrin, cells have ubiquitously expressed transferrin receptor 1 and 2 (TFR1 and TFR2). Upon binding, the TF-TFR complex undergoes endocytosis, through a clathrin dependent process, and the exposure to the acidic pH of the endosome releases iron from TF. Before entering the cytosol through DMT1, iron needs to be reduced from its ferric form by six-transmembrane epithelial antigen of prostate 3 (STEAP3) (Ohgami *et al.*, 2005). Then, the complex TF-TFR will be recycled, TF will return to the bloodstream and TFR1 will return to the cell surface (Fig. 2). The TF-TFR pathway is not the only way for iron to enter the cells as TFR1-independent iron uptake has been reported (Trinder *et al.*, 1996). For example, macrophages have various ways to import this metal, including phagocytosis of senescent erythrocytes (Bratosin *et al.*, 1998) or scavenging free hemoglobin or heme (Fig. 2). Iron scavengers, like haptoglobin and hemopexin, bind serum heme or hemoglobin that is released from ruptured erythrocytes. Macrophages are able to internalize these proteins and further degrade the heme group to obtain iron (Smith and McCulloh, 2015, Soares and Hamza, 2016) (Fig. 2). Once inside the cell, iron enters a pool of free iron, named labile iron pool (LIP), which consists in a transient pool of iron, alongside with some permeant chelators that prevent iron participation in the redox-cycling (Kakhlon and Cabantchik, 2002). From the LIP, iron can either be immediately used, stored inside the cell, or released through FPN1 (Delaby *et al.*, 2005, Van Zandt *et al.*, 2008) (Fig. 2).

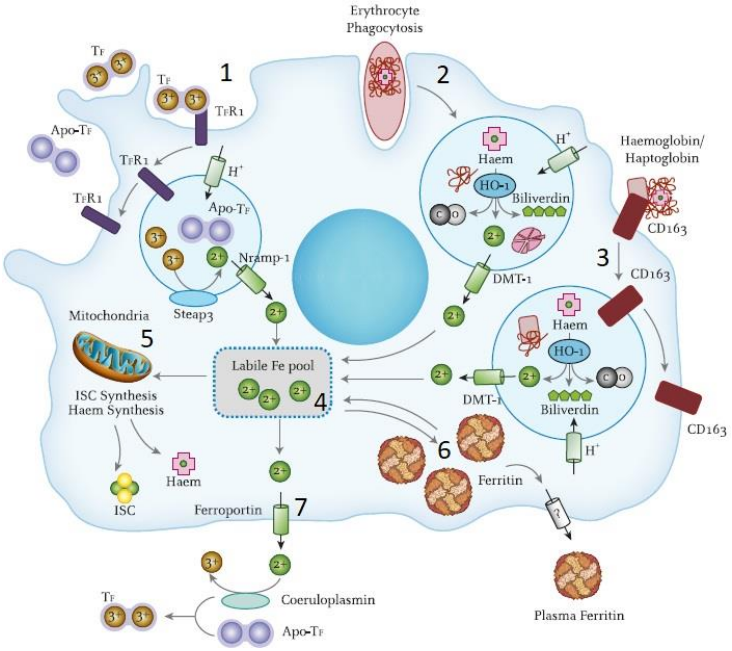

Figure 2 – Iron metabolism in macrophages. Iron can enter the cell through TF-TFR complex (1), erythrocyte phagocytosis (2), or heme and hemoglobin scavengers, like hemopexin and haptoglobin (3). (1) The TF-TFR complex enters the cells and releases iron through acidification of the endosome. TF is released from the cell and TFR goes back to the cell surface. Ferric iron is reduced by STEAP3 and enters the LIP with the help of natural resistance-associated macrophage protein-1 (NRAMP-1). (2,3) Erythrocytes, heme or hemoglobin scavangers are internalized by the cell, broken down inside lysosomes, releasing iron from heme through HMOX1, before joining the LIP. (4) From LIP, iron can either be used by (5) mitochondria for new heme synthesis, among others, (6) stored in ferritin or (7) exported by ferroportin. Adapted from (Evstatiev and Gasche, 2012).

The iron status of each cell is also regulated by iron responsive elements/iron regulatory proteins (IRE/IRP) that act in response to cellular iron content, affecting the expression of several iron-related proteins. This system impacts on iron acquisition (TFR1, DMT1), iron storage (H-ferritin [FTH1] and L-ferritin [FTL]), iron use (mitochondrial aconitase, hypoxia-inducible factor) and iron export ferroportin ([FPN1]) (Muckenthaler *et al.*, 2008).

Iron Regulatory Elements are a family of 28-nucleotide non-coding sequences present in mRNAs coding for some proteins involved in iron metabolism. Iron Regulatory Proteins bind to IRE, either preventing the degradation of the mRNA and increasing the production of the coded protein or blocking its translation (Fig. 3). IRP bind IRE only when cellular iron levels are low. When the IRP binds within the 5'UTR of the mRNA, translation is inhibited. This happens in genes coding for iron storage and iron export proteins as *Fth1*, *Ftl* and *Fpn1*. When the complex IRP-IRE is formed in the 3'UTR region, as occurs in mRNA coding for proteins involved in iron uptake as TFR or DMT1, the mRNA is stabilized preventing its degradation and increasing protein production (Daniels *et al.*, 2006, Torti and Torti, 2002) (Fig. 3).

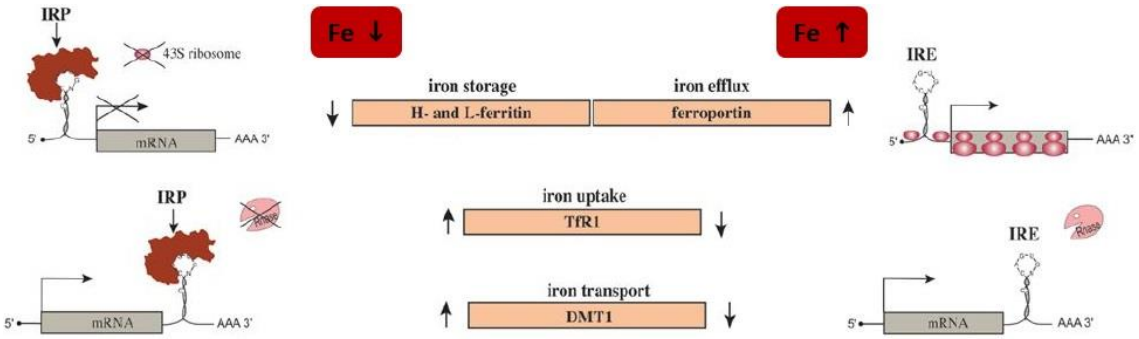

Figure 3 – Post-transcriptional control of cellular pathways by the IRE-IRP regulatory system. When in iron deplete conditions, IRP binds IRE within 5'UTR of mRNA, inhibiting H and L ferritin, and ferroportin translation, to lower iron storage and efflux; or bind IRE within 3'UTR stabilizing the mRNA of TFR1 and DMT1, enhancing iron uptake and transport. On the other hand, when iron levels are increased, IRP do not bind IRE, leading to opposite effects (higher iron storage and efflux and lower iron uptake and transport). Adapted from (Wang and Pantopoulos, 2011).

The Ferritin

Regarding the storage of iron in the cells, the key player on this process is ferritin. Ferritin is a large, spherical molecule that stores iron inside its core. This protein has been conserved throughout evolution in most living species, demonstrating the importance of ferritin and its functions. Ferritin is much more than an iron deposit, because it can protect the cells from the nefarious effects of free iron, and has been implied in immune regulation (Recalcati *et al.*, 2008, Theil, 1987). Generally, ferritin is a cytosolic protein, but has been described in mitochondria, nucleus and in serum (Levi *et al.*, 2001, Thompson *et al.*, 2002) (Levi et al., 2001). The cytosolic ferritin consists of a polypeptide with 24 protein subunits that compose

the apoferritin shell. This shell is capable of sheltering more than 4000 Fe^{3+} atoms and is composed of two types of subunits: H-ferritin (FTH1) and L-ferritin (FTL). These subunits are found at different ratios in the apoferritin shell, on different organs. In humans, the genes coding for the two proteins that make the apoferritin shell are located in different chromosomes, the H in the eleventh chromosome and the L in the nineteenth (Worwood *et al.*, 1985). In 1991 the structure of a ferroxidase moiety on the FTH1 protein was disclosed, leading to the understanding of the function on this subunit of ferritin (Lawson *et al.*, 1991). This ferroxidase is responsible for the conversion of Fe^{2+} to Fe^{3+} allowing ferritin to sequester iron inside the shell as a hydrous ferric oxide with a structure similar to the "ferrihydrite" (Chasteen and Harrison, 1999). This function is exclusively performed by the FTH1, since FTL does not have a ferroxidase center, making it incapable of oxidizing the iron. FTH1 is extremely important for the organism, as mice lacking *Fth1* gene cannot survive while embryos (Ferreira *et al.*, 2000).

Although FTL lacks the iron-oxidizing capacity, it has other functions. The presence of L chains in ferritin improves the stability of the protein helping the iron incorporation activity (Luscieti *et al.*, 2010). The electron transport that helps the mineralization and demineralization of iron on ferritin is also a specific function of the light chain (Carmona *et al.*, 2014). The H subunits of ferritin, as mentioned before, are the ones that will oxidize the iron making it possible to be stored inside the shell. This process can be complex. The Fe^{2+} enters ferritin with the help of an electrostatic gradient that attracts metal cations, and once internalized, the ferrous iron migrates to the ferroxidase center located on the heavy chain of ferritin. On this center, the Fe^{2+} atoms will react with hydrogen peroxide and will be oxidized into Fe^{3+} that, slowly, is going to be hydrolyzed and mineralized as ferrihydrite (Arosio *et al.*, 2015). These reactions protect the cell from the reactive species that can interact with other substrates and cause biological harm. Ferritin ensures that iron is immediately stored and detoxified, preventing the oxidative damage that could be caused by reactions like Haber-Weiss or Fenton.

As previously mentioned, ferritin can also be found in the serum (Wang *et al.*, 2010). The functions or effects of serum ferritin are not known. Serum ferritin can be taken up by cells but their putative receptors in humans and mice are distinct. In the mouse, T cell immunoglobulin-domain and mucin-domain (TIM), more specific TIM2, can serve as receptor to serum FTH1, but not FTL, while in humans the FTH1 receptor is the TFR1 and FTL can enter the cells through scavenger receptor class A member 5 (Chen *et al.*, 2005, Li *et al.*, 2009, Li *et al.*, 2010). Serum ferritin is thought to be a poor iron carrier but since each protein can carry more iron atoms than TF, it cannot be neglected as an iron delivery system. Serum ferritin is composed mainly by L subunits and very few H subunits (Cohen *et al.*, 2010). It was seen that both hepatocytes and macrophages have the ability to secrete ferritin, but the mechanisms by which this happens remain inconclusive (Ghosh *et al.*, 2004, Wang *et al.*, 2010).One of the hypothesis is that ferritin is secreted through a non-classical secretory pathway on a process

that starts on the endoplasmic reticulum. The ferritin accumulates in the lysosomal compartment being secreted through the secretory-lysosomal pathway (Cohen *et al.*, 2010).

Variations in the serum ferritin levels can be clinically relevant. Ferritin is used to estimate iron levels in the body, either to identify iron overload conditions or to distinguish between different types of anemia. There are other health problems where serum ferritin can help the diagnosis, from Still's disease to neurologic disorders and even cancer (Knovich *et al.*, 2009).

The macrophage

Macrophages have several functions throughout the body. Even though these cells are best known for their role in host defense, due to the ability to act against invading pathogens, this is just one of the many roles played by them. Macrophages are also important in wound repair and tissue homeostasis. Consistently, macrophages are key players in the iron homeostasis. Erythropoiesis is the most iron-demanding process in vertebrate animals. Since erythrocytes only have a lifespan on average of 120 days, macrophages have to "recycle" the iron on these cells in order to comply with iron demands. Conversely, macrophages help the formation of new red blood cells by providing them with the recycled iron and with a supportive niche in the bone marrow known as "erythroblastic islands" (Chow *et al.*, 2013).

Macrophages can either be tissue resident or bone marrow (BM)-derived. Tissue resident macrophages generally appear during embryogenesis and consist in groups of macrophages that populate different tissues, with different functions depending on site, and the ability of self-renewal (Davies *et al.*, 2013). These macrophages can be found in nearly every tissue, as in the liver (Kupfer cells) or in the spleen (red pulp macrophages) (Cumano and Godin, 2007). BM-derived macrophages are produced throughout life and are dependent of hematopoietic stem cells (HSC). HSC originate monocytes through a complex process involving several intermediate progenitor cells (Geissmann *et al.*, 2010). These monocytes can either stay as tissue resident macrophages in the bone marrow or disperse through the bloodstream to patrol the vascular endothelium or to aid in other tissues homeostasis (Zigmond and Jung, 2013).

Functions of the macrophage

Both tissue-resident macrophages and BM-derived macrophages have important and varied functions in different tissues. Macrophages are cells equipped to defend the organism against all sort of hazardous agents. Besides the ability of phagocytosing pathogens and inducing inflammation at the site of infection, macrophages can participate in the adaptive immunity by presenting antigens to T cells (Getz, 2005). Tissue-resident macrophages have different functions depending on their residence (Table 1). Kupffer Cells and red pulp macrophages have an upmost important role in iron metabolism. They phagocyte red blood cells recycling the heme molecule, releasing iron and making it available for further re–use (Kondo *et al.*, 1988,

Kurotaki *et al.*, 2015). In the BM, macrophages have key roles in numerous functions, as in the erythropoiesis or in the hematopoietic niche, supporting the HSC.

Table 1 - Tissue-resident macrophage and their functions (modified from (Varol *et al.*, 2015)).

Cell Type	Specific Organs to which Tissue Macrophage belongs	Function
Kupffer cell	Liver	Immunosurveillance Detoxification Iron and cholesterol recycling
Red pulp macrophage	Spleen	Immunosurveillance Detoxification Iron recycling Antigen delivery to DCs
Microglia	Brain	Immunosurveillance Clearing of cellular debris Synaptic pruning during development and adulthood
Peritoneal macrophage	Peritoneum	Immunosurveillance Support of IgA production by peritoneal B1 cells
Alveolar macrophage	Lungs	Immunosurveillance Support of IgA production by peritoneal B1 cells

Macrophages in iron metabolism

As was previously said, macrophages play a key role in the iron metabolism (Fig. 2). After RBC maturation, they have approximately 120 days in circulation, being removed by macrophages in the spleen and liver. Kupffer cells and red pulp cells are extremely important in this process, since they can phagocytose senescent and damaged erythrocytes (Kondo *et al.*, 1988, Kurotaki *et al.*, 2015). With the help of HMOX1, these macrophages remove the iron inside the heme group present in the erythrocytes (Fig. 2). This iron will return to the BM to be re-incorporated in the forming erythrocytes, and stored by ferritin. Macrophages can also release ferritin through exocytosis in order to "feed" iron to the erythroid precursors (EP) (Leimberg *et al.*, 2008). EP engulf ferritin, releasing iron intracellularly through acidification and proteolysis, making it available for heme synthesis (Leimberg *et al.*, 2008). Supplying iron to the EP is not the only way through which macrophages help the erythropoiesis. BM tissue-resident macrophages, known as nurse macrophages, support erythropoiesis by stimulating proliferation and survival of the erythroblast (nucleated red blood cell) (Chow *et al.*, 2013). Also, macrophages phagocytose and digest the nuclei of these cells with the help of DNase II (de Back *et al.*, 2014).

Macrophages also participate in the manipulation of iron metabolism aiming at the protection of the host against pathogenic agents (Cassat and Skaar, 2013). The main goal of this strategy is to deny iron to pathogens, leading to what is known by nutritional immunity (Soares and Hamza, 2016). In the case of extracellular pathogens, it will be beneficial to the host to lower the amount of iron found extracellularly, by storing it inside the cells. This can be achieved by either scavenging heme through haptoglobin and hemopexin, or by reducing FPN and inducing TFR and HMOX1 (Parrow *et al.*, 2013). The iron is then stored by ferritin. On the other hand, in the case of intracellular pathogens, like Mycobacteria, macrophages can try to deny iron either by suppressing heme entrance in the cell (TFR modulation) or increasing its release (through NRAMP-1 and DMT1). Iron already released from heme can either be exported by FPN or stored in ferritin. Release of iron from macrophages can lead to an induction in nitric oxide synthase (NOS2A) which contribute to the microbicidal activity of macrophages (Soares and Hamza, 2016).

The aim of this thesis' work is to study the role of FTH1, in BM-derived macrophage physiology. Since this protein is a key player in iron homeostasis, the cell viability and iron handling capacity will be the main focus of the study.

Chapter 2

Objectives

The main goal of this thesis work was to evaluate the role of FTH1 in macrophages biology. To achieve that we used a new experimental model consisting of mice with a conditional deletion of H-ferritin in cells of the myeloid lineage. We proposed to answer the following questions:

- **Is *Fth1* essential for the development and survival of BMM?**

- **Is the iron status of the macrophage influenced by the lack of *Fth1*?**

- **What is the role of *Fth1* in macrophages response to exogenous iron?**

- **How does *Fth1* impact in the macrophages response to immune and microbial stimuli?**

Chapter 3

Materials and Methods

Chemicals

In general, all chemicals used were obtained from Sigma Aldrich (Sto Louis, MO, USA), unless specified. Particularly, for cell culture, the reagents were obtained from Gibco (Paisley, U.K.); for protein extraction, western blot and qPCR were obtained from Bio-Rad (Hercules, CA, USA); and flow cytometry antibodies were obtained from Biolegend, San Diego, CA, USA, unless stated otherwise. Phosphate buffered saline (PBS) was prepared in water with 9% sodium chloride (NaCl), 1.1% sodium hydrogen phosphate (Na_2HPO_4) and 0.2% potassium dihydrogen phosphate (KH_2PO_4).

Animals

Conditional *Fth1* deficient (*Fth1*$^{Fl/Fl}$*; Lyz2*$^{cre/+}$) mice, obtained by crossing *Lyz2*$^{cre/+}$ mice with *Fth1*$^{Fl/Fl}$ mice were kindly provided by Prof. Lukas Kuhn (Swiss Institute for Experimental Cancer Research, Lausanne, Switzerland) (Darshan, Vanoaica, Richman, Beermann, & Kühn, 2009). In these mice, Cre recombinase deletes the *Fth1* gene in cells expressing *Lyz2* (cells of the myeloid lineage). *Fth1*$^{Fl/Fl}$*; Lyz2*$^{+/+}$ (Cre^{-}) littermate mice were used as experimental controls. The experiments described in this thesis were carried out with male mice between 12 to 18 weeks-old. All procedures were performed with the approval of Direção-Geral de Alimentação e Veterinária (DGAV), the Portuguese National Authority for Animal Health, and the persons involved in the experiments were credited for animal experimentation by FELASA (Federation for Laboratory Animal Science Associations) at levels B or C

Bone marrow-derived macrophages

Bone Marrow-derived Macrophages (BMM) were obtained from the bone marrow of the femur and tibia of the *Fth1*$^{Fl/Fl}$*; Lyz2*$^{+/+}$ and *Fth1*$^{Fl/Fl}$*; Lyz2*$^{cre/+}$ mice. The cells obtained were either sufficient (Mo-*Fth1*$^{+/+}$) or deficient (Mo-*Fth1*$^{-/-}$) in H-ferritin, respectively. The animals were sacrificed with isoflurane anesthesia followed by cervical dislocation, and both femurs and tibias were harvested. The bones were flushed with cold Hank's Balanced Salt Solution (HBSS) centrifuged and resuspended with Dulbeccos's Modified Eagle Medium (DMEM) supplemented with 1 M HEPES, 200 mM L-glutamine, 100 mM sodium pyruvate, 10% inactivated fetal bovine serum (FBS) (Gibco or Biowest, France) and 10% of L929 cell conditioned medium (LCCM) as a source of Macrophage Colony Stimulating Factor (M-CSF). Cells were cultured overnight at 37

^{o}C, 7% CO_2 in a Nuclon plate (Thermo Fisher, Massachusetts, USA). Afterwards, the non-adherent cells were collected with cold HBSS, centrifuged, resuspended with DMEM/10%LCCM to a density of $4x10^5$ cells/ml and seeded onto culture plates. At the 4th day of culture 10% LCCM was added, and at the 7th day the whole medium was renewed.

Cell morphology

To evaluate if the two genotypes would have differences in cell morphology, cells were imaged every 24 h, during an entire experiment, to evaluate growth and morphology. The cells were visualized and photographed in an inverted optical microscope (Olympus SC30).

Cell viability

Cell metabolic activity:

Cell metabolic activity was measured by resazurin reduction. Briefly, 10% (v/v) of resazurin (0,3 mg/ml) was added to the cells and incubated for 20 h. The fluorescence of resorufin, resulting from the reduction of resazurin by metabolic active cells, was measured at λ_{ex}=530 nm λ_{em}=590 nm in Synergy™ Mx (BioTek, Winooski, VT, USA).

Cell membrane permeability:

In order to assess cell membrane permeability, cells were washed with warm 5%FBS/PBS, and incubated with a mixture of a cell-permeable nuclear dye, for cell counting (Hoechst 33342, 1:12000, Invitrogen, Eugene, OR, USA) and a membrane-impermeable dye SYTOX™ Green (1:45000, TermoFisher, Waltham, MA, USA), for 20 minutes at 37 ^{o}C and 7% CO_2, and washed again. The cells were visualized and photographed in a controlled environment (37 ^{o}C, CO_2 atmosphere) with a 20x Nikon objective in a high-throughput automated fluorescence wide field microscope (IN Cell Analyzer 2000, GE Healthcare, Little Chalfont, UK). The images were then analyzed with Developer Toolbox 1.9.2 (GE Healthcare, Little Chalfont, UK).

Flow cytometry

To perform flow cytometry, the cells were collected at the 7th and 10th day of culture, labelled with anti-mouse CD11b and anti-mouse F4/80 antibodies (1:200 and 1:100, respectively) in FACS buffer (1%FBS/PBS), and conjugated with AmCyan-A and APC-Cy7-A as fluorochromes, respectively. The samples were washed, the supernatant discarded and cells resuspended in FACS buffer. Samples were then analyzed using the BD FACSCanto™ II Bioanalyser (BD Biosciences, San Jose, CA, USA) and with FlowJo software (FlowJo, LLC, USA). Cells were initially gated based on the size (forward scatter, FSC) and granularity (side scatter, SSC),

allowing single cells to be selected. Double positive cells for F4/80 and CD11b were considered fully differentiated macrophages.

Cell-treatments

Iron treatments were given to the cells at the 7th day of culture (day 0 post-treatment), at different concentrations (0.1, 0.25, 0.5, 1, 5, 10, 15, 30, 60, 100, 200, 300, 400 and 600 μM). The iron compounds used were, ferric ammonium citrate (FAC), hemin (Frontier Scientific Inc, Logan, UT, USA) and an iron chelator, desferoxamine B mesylate (DFO). FAC and DFO were dissolved in PBS, and hemin was prepared as previously described (Silva-Gomes, et al., 2013). Briefly, hemin was dissolved in NaOH 0.2 M, the pH was adjusted to 7.4, and the volume was made up with distilled water. Recombinant mouse Interferon gamma (IFN-γ) (Gibco, MD, USA) was added at 16 ng/ml, at the 7th day of culture (day 0 post-treatment), and 2 more times with a 24 h range. Lipopolysaccharide (LPS) was given at 10 ng/ml and diluted in DMEM/10%LCCM. Cell viability and morphology were evaluated 72 h after treatments, as described above.

TUNEL

Terminal deoxynucleotidyl transferase dUTP nick end labeling (TUNEL) assay was performed following manufacturer's instructions (Roche, Basel, Switzerland). Briefly, 72 h post-treatment, cells were fixed with 4% paraformaldehyde (PFA) in PBS for 15 minutes, washed with PBS and incubated with permeabilisation solution (0.1% Triton X-100 in 0.1% sodium citrate) for 2 minutes at 4 ºC. Afterwards, each sample was labelled with 50 μl of TUNEL reaction mixture (5 μl of TUNEL-Enzyme with 45 μl TUNEL-Label) and incubated for 1 h at 37 ºC in a humidified chamber in the dark. The cells were visualized and photographed with a 20x Nikon objective in a high-throughput automated fluorescence wide field microscope (IN Cell Analyzer 2000, GE Healthcare, Little Chalfont, UK). The images were then analyzed with Developer Toolbox 1.9.2 (GE Healthcare, Little Chalfont, UK).

ELISA

Mouse TNF-α ELISA Ready-SET-Go was performed following manufacturer's instructions (TermoFisher, Waltham, MA, USA). First, Nunc Maxisorp® plates were coated with capture antibody (anti-mouse TNF-α purified) diluted in Coating buffer overnight. Afterwards, the plates were washed with wash buffer (0.05% Tween-20/PBS), blocked with Assay Diluent for 1 h at room temperature, and incubated with standards (Mouse TNF-α recombinant proteins) or samples (cells' supernatants at 72 h of incubation with treatments), overnight at 4 ºC. Detection antibody (anti-mouse TNF-α Biotin), diluted in Assay Diluent, was incubated for 1 h at room temperature, followed by Avidin-HRP for 30 minutes at room temperature, substrate solution for 15 minutes at room temperature, and finally, stop Solution (1 M H_3PO_4). The absorbance

was read at 450 nm and 570 nm (for subtraction), on a μQuant™ Microplate Spectrophotometer (BioTek Instruments, Winooski, VT, USA).

Griess

To evaluate nitrites production, Griess assay was performed using the cells' supernatant. After 72 h of incubation with the different treatments, the medium was recovered, and incubated with Griess reagent (1% sulfanidamine, 0.1% naphthylenediamine dihydrochloride (NEDADHC), 1.72% phosphoric acid 85%, in water) in a proportion of 1:1, for 10 minutes. The standard curve was made using sodium nitrite ($NaNO_2$). After incubation, the absorbance was read at 550 nm on a μQuant™ Microplate Spectrophotometer (BioTek Instruments, Winooski, VT, USA).

Protein extraction

All the procedures were performed at 4 ºC. The cell culture medium was collected and cells were harvest with 5 mM ethylenediaminetetraacetic (EDTA)/PBS. Cells were then centrifuged and washed with cold PBS followed by another centrifugation. Afterwards, the cells were resuspended with collecting buffer (Ripa buffer: 150 mM NaCl, 1.0% NP-40, 0.5% sodium deoxycholate, 0.1% SDS, 50 mM Tris, pH 8.0), supplemented with dithiothreitol (DTT), phenylmethylsulfonyl fluoride (PMSF) and a protease inhibitor cocktail, followed by rupture with a 26–gauge needle. The protein suspension was then stored at -80 ºC, prior sample quantification (with DC™ protein assay) and preparation for western blot.

Western blot

Equivalent amounts of protein prepared in Laemmli buffer were separated by electrophoresis (30 mA per gel, with 10% SDS polyacrylamide gels (SDS-PAGE)) and electrophoretically transferred into an activated (methanol 10 seconds, water 5 minutes and transfer buffer for 15 minutes) polyvinylidene difluoride (PVDF) membrane for 90 min at 100 V. Membranes were blocked with 5%BSA in tris-buffered saline with Tween20 (TBS-T) (NaCl 150 mM, Tris 50 mM, Tween-20 0.1%) for 1 h at room temperature, followed by overnight incubation with the primary antibodies (FTH1, 1:500, Cell Signaling Technology, Danvers, MA, USA; ß-actin, 1:5000, Abcam, Cambridge, UK) prepared in 1% bovine serum albumin (BSA)/TBS-T. The membranes were washed with TBS-T, and incubated with the secondary antibody (anti-rabbit, 1:10000, The Binding Site, Birmingham, UK) in 1%BSA/TBS-T for 1 h at room temperature. The imaging of the membranes was made using ChemiDoc (Bio-Rad, Hercules, CA, USA), with the help of horseradish peroxidase (HRP) (Luminata™ Milipore, Billerica, MA, USA) substrate. Membrane analysis was performed with ImageLab™ software (Bio-Rad, Hercules, CA, USA).

RNA extraction

In order to extract RNA from the BMM we used PureLink® RNA Mini Kit, following the manufacturer's instructions (Ambion™, Invitrogen, Carlsbad, CA, USA). Briefly, lysis buffer, supplemented with 1% ß-mercaptoethanol, was added to the cells and samples were homogenized for 45 seconds. The centrifuged supernatant was transferred to a new tube and the same volume of ethanol 70% was added. After mixing, the whole volume was transferred to the mini-columns. The next step was to centrifuge at 1200 g for 15 seconds after a wash with "wash buffer I" and two washes with "wash buffer II". The extracted RNA was eluted with RNAse-free water from the column to a proper tube. The samples were stored at -80 ºC, prior to conversion to cDNA and qPCR analysis.

qPCR

Table 2 – Primers list.

Gene	Sequence
***Hprt* forward**	5'-GGTGGAGATGATCTCTCAAC-3'
Hprt reverse	5'-TCATTATAGTCAAGGGCATATCC-3'
***Fth1* forward**	5'-GCTGAATGCAATGGAGTGTGCA-3'
***Fth1* reverse**	5'-GGCACCCATCTTGCGTAAGTTG-3'
***Ftl* forward**	5'-ACCTACCTCTCTCTGGGCTT-3'
***Ftl* reverse**	5'-TGGCTTCTGCACATCCTGGA-3'
***Slc40a1* forward**	5'-TTGGTGACTGGGTGGATAAGAATGC-3'
***Slc40a1* reverse**	5'-CGCAGAGGATGACGGACACATTC-3'
***Hmox1* forward**	5'-GCCACCAAGGAGGTACACAT-3'
***Hmox1* reverse**	5'-GCTTGTTGCCCTCTATCTCC-3'
***Tfrc* forward**	5'-GCAGCATTGGTCAAAACATGG-3'
***Tfrc* reverse**	5'-GCTTTGGGCATTTGCAACCC-3'
***Nos2a* forward**	5'-ACATCGACCCGTCCACAGTAT-3'
***Nos2a* reverse**	5'-CAGAGGGGTAGGCTTGTCTC-3'
***Arg1* forward**	5'-CTCCAAGCCAAAGTCCTTAGAG-3'
***Arg1* reverse**	5'-CGAGCTGTCATTAGGGACATCA-3'
***Tnf* forward**	5'-CCGTCAGCCGATTTGCTATCT-3'
***Tnf* reverse**	5'-CGGACTCCGCAAAGTCTAAG-3'

The RNA was converted into cDNA with the First-Strand cDNA Synthesis Kit (NZYtech, Lisbon, Portugal) following the manufacturer's instructions. The cDNA was stored at -20 ºC before use. To perform the qPCR, the samples were prepared with the probe (iTaq Universal SYBR Green – Bio-Rad, Hercules, CA, USA), and a specific pair of primers (forward and reverse) (Table 2). The qPCR was made on IQ5 (Bio-Rad, Hercules, CA, USA), where the cDNA was heated 5 minutes at 94 ºC and entered a cycle that repeated 24 times the following: heat 30 seconds at 94 ºC, 1 minute at 30 ºC and 30 seconds at 72 ºC. At the end of the cycle, the sample was heated for 5 minutes at 72 ºC, and kept at 4 ºC. Threshold cycles (CT) were obtained by the Bio-Rad iQ™5 software and normalized to the housekeeping gene, hypoxanthine guanine phosphoribosyl transferase (*Hprt1*) (ΔCT) (equation 1). Then, ΔCT was used to calculate ΔΔCT which was

further used to determine the n-fold difference relative to non-treated samples of Mo-*Fth1*$^{+/+}$, calculated with $2^{-\Delta\Delta CT}$ (equation 2).

$$\Delta CT \text{ (x or y)} = CT_{goi} - CT_{gor} \qquad (1)$$

$$2^{-\Delta\Delta CT} = 2^{-(\Delta CT\ x\ -\ \Delta CT\ y)} \qquad (2)$$

goi – gene of interest; gor – gene of reference; x – goi from non-treated or treated Mo-*Fth1*$^{+/+}$ or Mo-*Fth1*$^{-/-}$; y – goi from non-treated Mo-*Fth1*$^{+/+}$.

Data analysis

The concentration of FAC, hemin and DFO that inhibits 50% of the macrophage viability (IC_{50}) was determined by fitting the resazurin data with a four-parameter dose-response sigmoidal curve using GraphPad Prism 7 software (GraphPad Software, Inc, La Jolla, CA, USA).

Statistical analysis was performed as described in the figures' legends using GraphPad Prism 7 (GraphPad Software, Inc, La Jolla, CA, USA). Statistical significance was obtained when $p < 0.05$.

Chapter 4

Results

1. Mo-*Fth1*$^{-/-}$ develop normally from their precursors in the bone marrow

1.1. The viability of BMM is the same regardless of the expression of *Fth1*

In order to evaluate the effect of the lack of *Fth1* on macrophage differentiation from their precursors, BM cells were extracted from *Fth1*$^{Fl/Fl}$; *Lyz2*$^{+/+}$ and *Fth1*$^{Fl/Fl}$; *Lyz2*$^{cre/+}$ mice in order to obtain sufficient (Mo-*Fth*$^{+/+}$) and deficient (Mo-*Fth*$^{-/-}$) macrophages in H-ferritin. BMM viability was evaluated through resazurin reduction. Resazurin is a blue non-fluorescent dye capable of permeating the cell membrane. Once inside the cell, it can be reduced into resorufin (pink and fluorescent) by viable cells with active redox metabolism. As can be seen in figure 4, the cells' viability did not differ between the two genotypes regardless of the day of culture.

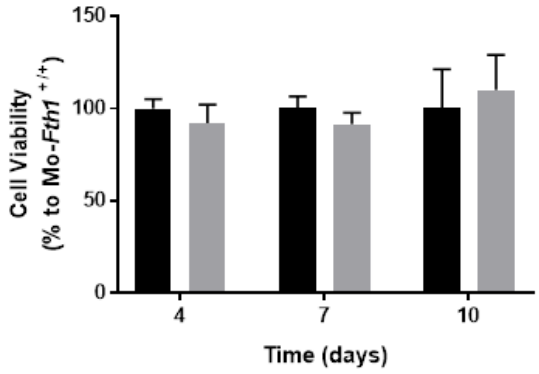

Figure 4 – BMM viability is not dependent of *Fth1* expression. Cell viability of Mo-*Fth1*$^{+/+}$ (black bars) and Mo-*Fth1*$^{-/-}$ (grey bars) was measured at 4, 7 and 10 days after the beginning of the culture. At those time-points, resazurin 0.3 mg/ml was added at 10% (v/v) and after 20 h the fluorescence was measured at 530/590 nm. The graphs represent the mean + standard deviation (SD) (n[Mo-*Fth1*$^{+/+}$] = 7; n[Mo-*Fth1*$^{-/-}$] = 14).

1.2. Mo-*Fth1*$^{-/-}$ express the same levels of macrophage surface markers than Mo-*Fth1*$^{+/+}$

At different time-points (7th and 10th days), the development and differentiation of the cells in culture were evaluated by flow cytometry, using the cells' size and granulosity and two well-known macrophages' surface markers: F4/80 and CD11b. F4/80 is a well-characterized membrane protein and is a homolog to epidermal growth factor (EGF)-like module-containing

mucin-like hormone receptor-like 1 (EMR1) of humans. This protein is used as a macrophage marker since 1981, when it was found that it was expressed during macrophage differentiation in culture (Austyn and Gordon, 1981). CD11b, also known as macrophage-1 antigen (Mac-1), is a macrophage cell surface antigen, of the integrins' family (Podolnikova *et al.*, 2016).

The results obtained from flow cytometry analysis indicate that both Mo-*Fth1*$^{+/+}$ and Mo-*Fth1*$^{-/-}$ mature similarly, as there were almost no differences in the markers' expression and cells' size (Fig. 5). Besides, at the 7th day of culture both macrophages genotypes (93% - Mo-*Fth1*$^{+/+}$ and 92% - Mo-*Fth1*$^{-/-}$) had already matured (meaning the macrophages have differentiated) from their precursors. Since, in both cultures, the cells had matured at this time-point, subsequent experiments were performed 7 days after the beginning of the culture.

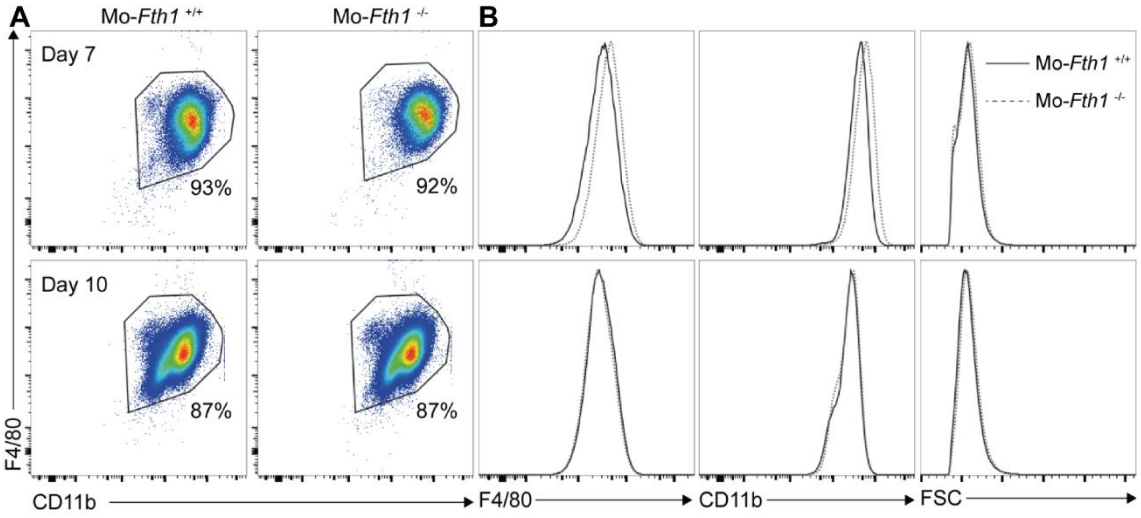

Figure 5 - H-ferritin deficiency does not impact macrophage differentiation. At days 7 and 10 of culture, BMM were stained for the myeloid markers F4/80 and CD11b and analyzed by flow cytometry. A) Flow cytometry plots of CD11b and F4/80 staining of Mo-*Fth1*$^{-/-}$ and Mo-Fth1$^{+/+}$ at the two time-points. Percentages indicate the frequency of CD11b+ F4/80+ cells. B) Histogram plots of Mo-*Fth1*$^{-/-}$ (dotted grey line) and Mo-*Fth1*$^{+/+}$ (solid black line) for F4/80 (left panel) and CD11b (middle panel) markers, and cell size (FSC, right panel). One representative experiment out of two is shown.

1.3. The morphology of *Mo-Fth1*$^{-/-}$ and *Mo-Fth1*$^{+/+}$ are undistinguishable

To analyze cell morphology, the cultures were imaged once a day during the entirety of the experiment. From the first day to the 8th day, the cells started from a round shape to a more flattened one (Fig. 6A). Another difference visualized was the cells' enlargement during maturation, starting to gain filamentous protrusions extending from the main body. The changes described, happened to both Mo-*Fth1*$^{+/+}$ and Mo-*Fth1*$^{-/-}$ at the same time. From the 8th day to the last day of culture (10th day), changes in morphology, were less visible (Fig. 6B). There was a loss of cell density, and some macrophages start to gain a rounder shape again. The number of cell ramifications increased with time. These phenotypes seem to be occurring in the two genotypes, as there were no significant differences between them.

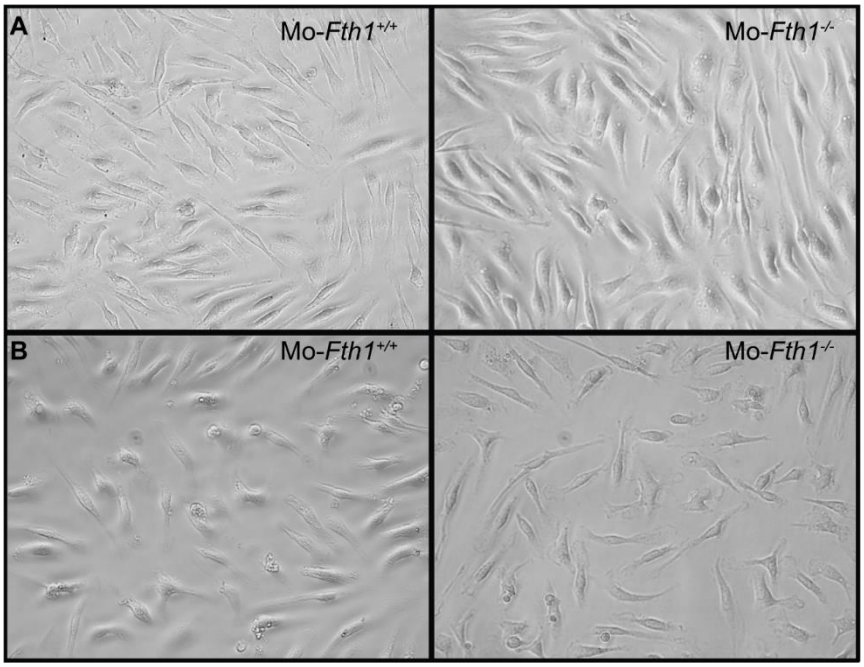

Figure 6 – Mo-*Fth1*$^{-/-}$ and Mo-*Fth1*$^{+/+}$ have similar morphologies. Light microscopy images of BMM at **A)** 8 and **B)** 10 days after the beginning of the culture. Pictures shown here are representative of four independent experiments. The cells were visualized and photographed in an Olympus SC30 camera.

1.4. FTH1 is not expressed in Mo-*Fth1*$^{-/-}$

The animal model used in these studies was designed so that the *Fth1* gene is deleted in all cells of the myeloid lineage. In order to confirm that there was no expression of FTH1 in Mo-*Fth1*$^{-/-}$ western blot analysis for this protein was performed at the 10th day of culture. The results confirmed that FTH1 was absent from *Mo-Fth1*$^{-/-}$ (Fig. 7).

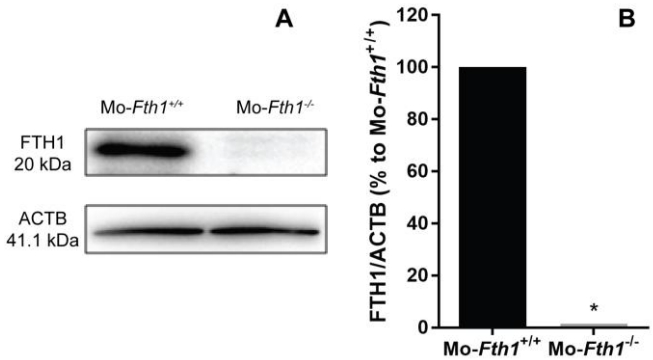

Figure 7 – Mo-*Fth1*$^{-/-}$ do not express H-Ferritin. A) 10 days after the beginning of the culture, BMM were harvested, total protein quantified and H-ferritin (FTH1) expression was determined by Western blot. ß-actin (ACTB) was used as housekeeping protein (loading control). These results are representative of two independent experiments. **B)** The graph represents the densitometry analysis obtained with ImageLab™ software of FTH1 expression in each culture, normalized to ACTB densitometry, expressed as percentage to Mo-*Fth1*$^{+/+}$. Statistical analysis was performed using an unpaired t test. * $p < 0.05$ statistically significant.

2. The lack of *Fth1* alters the way macrophages deal with iron.

2.1. Basal expression of iron related genes does not change between genotypes

H-ferritin is a key player in iron metabolism. Thus, its deletion should impact the whole circuit and the other key components expression. To evaluate this, at the last day of the culture (10th day), RNA was extracted and transcribed into cDNA. Then, through qPCR, expression levels of some iron metabolism related genes were determined. Surprisingly, no significant changes happened in the expression of all tested genes, with the exception of *Fth1* (Fig. 8).

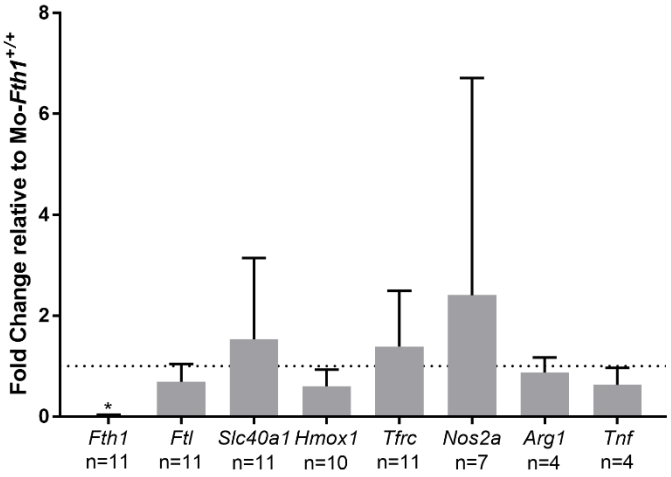

Figure 8 – **Expression of iron metabolism genes are similar in both genotypes.** 10 days after the beginning of the culture, qPCR was used to determine the expression levels of several genes involved in iron metabolism: H-ferritin *(Fth1)*, L-ferritin (*Ftl*), ferroportin (*Slc40a1*), heme oxygenase 1 (*Hmox1*), transferrin receptor (*Tfrc*), inducible nitric oxide synthase *(Nos2a)*, arginase (*Arg1*) and tumor-necrosis factor (*Tnf*). Data represent the mean + SD are expressed as the fold-change of expression in Mo-*Fth1*$^{-/-}$ (grey bars) relative to that in Mo-*Fth1*$^{+/+}$ (dashed line). Number of samples for each gene is depicted in the graph. Statistical analysis was performed using unpaired t-test. * $p < 0.05$ statistically significant.

2.2. When treated with exogenous iron, Mo-*Fth1*$^{-/-}$ loose viability to a higher extent than Mo-*Fth1*$^{+/+}$

Although Mo-*Fth1*$^{-/-}$ cells had apparently normal iron-related gene expression, we hypothesized that these cells should not be capable of handling exogenous iron as well as Mo-*Fth1*$^{+/+}$. Exogenous iron and an iron chelator were given to the cells' medium at the 7th day of culture ranging within different concentrations: hemin (0.5 µM – 600 µM), ferric ammonium citrate (FAC) (0.1 µM – 400 µM) and desferoxamine (DFO) (0.1 µM – 600 µM). Viability of the cells was evaluated by resazurin reduction assay, at the 10th day of culture (3 days post-treatment). As expected, FAC and hemin caused a concentration-dependent reduction of cell viability in both types of macrophages. Interestingly, in the presence of 5 to 400 µM concentrations of FAC (Fig. 9A) and of 15 to 300 µM of hemin (Fig. 9B) the viability of the Mo-*Fth1*$^{-/-}$ was significantly lower

than Mo-*Fth1*$^{+/+}$. In accordance, the IC_{50} of these compounds for Mo-*Fth1*$^{-/-}$ were several folds lower than for Mo-*Fth1*$^{+/+}$ (Table 3). The IC_{50} was measured using GraphPad Prism 7 software, calculating the nonlinear regression of the data. But since our values do not reach the lowest value possible (0% viability), we constrained the bottom value, present in the formula used to calculate the IC_{50}, to 0, leaving the top value to be the highest value we obtained. While dealing differently with exogenous iron, the same behavior was not observed when given the iron chelator DFO (Fig. 9C). Plus, since the values of viability drop to 50% at 10 µM and remain like this up to the highest concentration tested (600 µM), it was not possible to calculate the IC_{50} for this compound.

Table 3 - Iron toxicity in Mo-*Fth1*$^{-/-}$ and Mo-*Fth1*$^{+/+}$.

Compounds	IC_{50} ± SD (µM)	
	Mo-*Fth1*$^{+/+}$	Mo-*Fth1*$^{-/-}$
FAC	**26.6 ± 1.2**	**9.7 ± 1.1**
Hemin	150.9 ± 1.1	49.6 ± 1.0

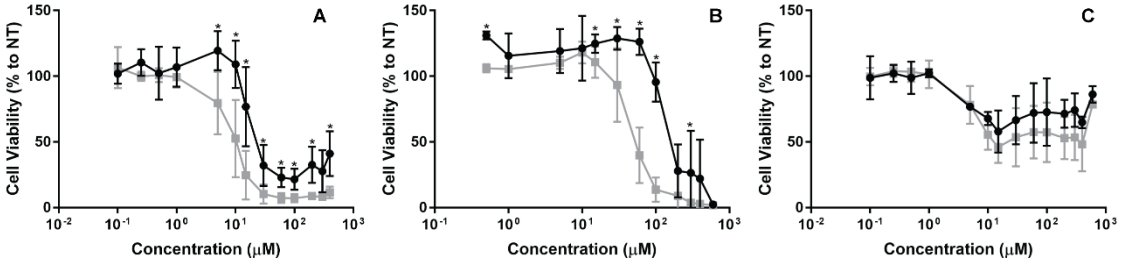

Figure 9 - Mo-*Fth1*$^{-/-}$ are more sensitive to iron toxicity. Mo-*Fth1*$^{+/+}$ (black) and Mo-*Fth1*$^{-/-}$ (grey) were treated with FAC (**A**), hemin (**B**) or the iron chelator DFO (**C**) at different concentrations, 7 days after the beginning of the culture. Cell viability was measured 3 days later, by resazurin reduction: resazurin (0.3 mg/ml) was added at 10% (v/v), incubated for 20 h, and the fluorescence was measured at 530/590 nm. The graphs represent the mean ± SD (n[Mo-*Fth1*$^{+/+}$] = 3; n[Mo-*Fth1*$^{-/-}$] = 7). Statistical analysis was performed using two-way ANOVA with Tukey's multiple comparisons. * $p < 0.05$ statistically significant.

To further confirm these results, we analyzed cell death using SYTOXTM Green and TUNEL assay. SYTOXTM Green is a cell-impermeable stain with high affinity to nucleic acids that can only penetrate the cells with compromised membrane, but cannot pass the membrane of intact cells. When SYTOXTM Green binds to DNA it increases its fluorescence intensity. After 72 hours of incubation with the different treatments, SYTOXTM Green was added to the cells. Both iron compounds caused significantly more cell death in Mo-Fth1-/- when compared to Mo-Fth1+/+ (Fig. 10A-B). With FAC, this difference was evident from 5 µM to the highest concentration tested (100 µM), although at 10 µM there was no significant difference between the cell types (Fig. 10A). With hemin, differences were evident only at concentrations of 100 µM and 200 µM (Fig. 10B). Once again, DFO did not lead to significant differences between the two genotypes (Fig. 10C).

TUNEL assay is a method used to detect cell death through DNA fragmentation, which is a hallmark of apoptosis. The cells were fixed 72 h after incubation with treatments and proceeded for analysis with the TUNEL assay. Although this assay was only performed once, there was a clear difference in apoptotic death between the two BMM genotypes (Fig. 10D). With FAC (30 μM) Mo-*Fth1*$^{-/-}$ had 23% of cell death against the 3% of Mo-*Fth1*$^{+/+}$, while with hemin (100 μM) Mo-*Fth1*$^{-/-}$ had 91% of cell death against 5% of Mo-*Fth1*$^{+/+}$. DFO (100 μM) did not cause significant death either on Mo-*Fth1*$^{-/-}$ (2% cell death) or on Mo-*Fth1*$^{+/+}$ (1% cell death) (Fig 10C-D).

Taking into account all these results, *Mo-Fth1*$^{-/-}$ seem to be less capable of handling exogenous iron, being more sensitive to iron-induced cell death.

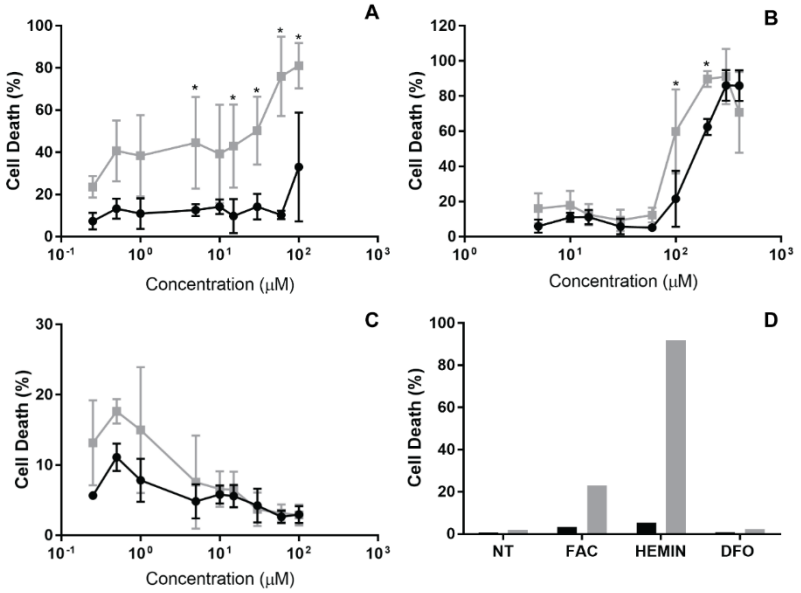

Figure 10 – Cell viability of Mo-*Fth1*$^{-/-}$ decreases in the presence of iron. Mo-*Fth1*$^{+/+}$ (black) and Mo-*Fth1*$^{-/-}$ (grey) were treated with FAC (**A**), hemin (**B**) or the iron chelator DFO (**C**) at different concentrations, 7 days after the beginning of the culture. Cell death was measured through SYTOX™ Green three days after the treatment. The graphs represent the mean + SD (n[Mo-*Fth1*$^{+/+}$] = 2; n[Mo-*Fth1*$^{-/-}$] = 4). Statistical analysis was performed using two-way ANOVA with Tukey's multiple comparisons. * $p < 0.05$ statistically significant. (**D**) Cell death was analyzed through TUNEL assay. Mo-*Fth1*$^{+/+}$ (black) and Mo-*Fth1*$^{-/-}$ (grey) were treated with 30 μM FAC, 100 μM hemin and 100 μM DFO, for 72 h. The graph represents one experiment (n[Mo-*Fth1*$^{+/+}$] = 1; n[Mo-*Fth1*$^{-/-}$] = 1).

3. The lack of *Fth1* has a minor impact on BMM response to cytokine or microbial activation

Interferon-γ (IFN-γ) and lipopolysaccharide (LPS) are known activators of macrophage's antimicrobial mechanisms. IFN-γ is mostly produced by natural-killer cells and T cells. LPS is a component of the outer membrane of Gram negative bacteria. Both molecules can activate the macrophage and are important for the innate immunity of the organism. Therefore, we wanted

to evaluate the differences between *Mo-Fth1*$^{+/+}$ and *Mo-Fth1*$^{-/-}$ in an activation scenario. At the 7th day of culture, IFN-γ, LPS or IFN-γ+LPS were added to the cells' cultures. At the 10th day (3 days post treatments), we assessed the cellular viability by resazurin and SYTOX™ Green assays, and we observed that only IFN-γ had an impact on cell viability and death in Mo-*Fth1*$^{-/-}$ (Fig. 11).

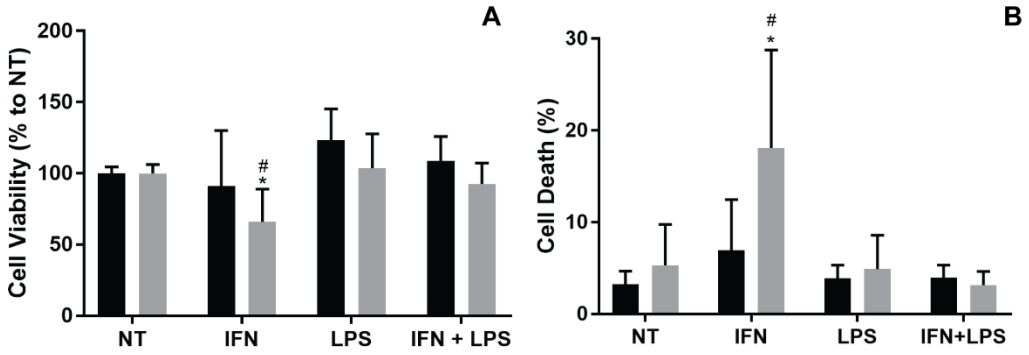

Figure 11 - Mo-*Fth1*$^{-/-}$ have an increased susceptibility to IFN-γ. Cells were treated with IFN-γ, LPS or IFN-γ+LPS, 7 days after the beginning of the cell culture. Cell viability (A) and cell death (B) of Mo-*Fth1*$^{+/+}$ (black) and Mo-*Fth1*$^{-/-}$ (grey) were measured 3 days after treatments. A) Resazurin (0.3 mg/ml) was added at 10% (v/v), incubated for 20 h, and fluorescence was measured at 530/590 nm. The graph represents the mean + SD of five independent experiments (n[Mo-*Fth1*$^{+/+}$] = 3; n[Mo-*Fth1*$^{-/-}$] = 7). B) Cell death was measured through SYTOX™ Green. The graph represents the mean + SD (n[Mo-*Fth1*$^{+/+}$] = 2; n[Mo-*Fth1*$^{-/-}$] = 4). * $p < 0.05$ when comparing the two genotypes. # $p < 0.05$ statistically significant when comparing with the corresponding NT sample.

We have also evaluated the expression of several genes known to respond to IFN-γ and/or LPS. As expected, Mo-*Fth1*$^{-/-}$ had very low expression of *Fth1*, which did not significantly increase with the treatments. Mo-*Fth1*$^{+/+}$ increased their expression of *Fth1* when treated with LPS. Regarding *Ftl*, no relevant changes in gene expression were observed (Fig. 12A and B).

The treatments caused a decrease in the expression of *Slc40a1* in both genotypes. Conversely, expression of *Tfrc* tended to increase with treatment in Mo-*Fth1*$^{+/+}$, but not in Mo-*Fth1*$^{-/-}$ (Fig. 12C and E).

Hmox1 is a gene known to be induced in macrophages by microbial products. Our results show that when in presence of IFN-γ+LPS both cell types expressed *Hmox1* several folds more (Fig. 12D).

Induction of *Nos2a* expression is a hallmark of macrophage activation. We observe the induction of *Nos2a* expression in macrophages treated either with IFN-γ, LPS or both. Interestingly, the induction of *Nos2a* upon treatment with IFN-γ+LPS was significantly lower in *Mo-Fth1*$^{-/-}$ when compared to *Mo-Fth1*$^{+/+}$ (Fig. 12F). Accordingly, there was also significantly lower production of nitrites by *Mo-Fth1*$^{-/-}$ than *Mo-Fth1*$^{+/+}$ (Fig.13A), indicating that the lack of *Fth1* somehow impairs *Nos2a* expression and activity. To evaluate another marker of macrophage activation,

TNF-α was measured by ELISA. Although LPS and IFN-γ+LPS increased TNF-α, we found no significant differences between the two cell types (Fig. 13B).

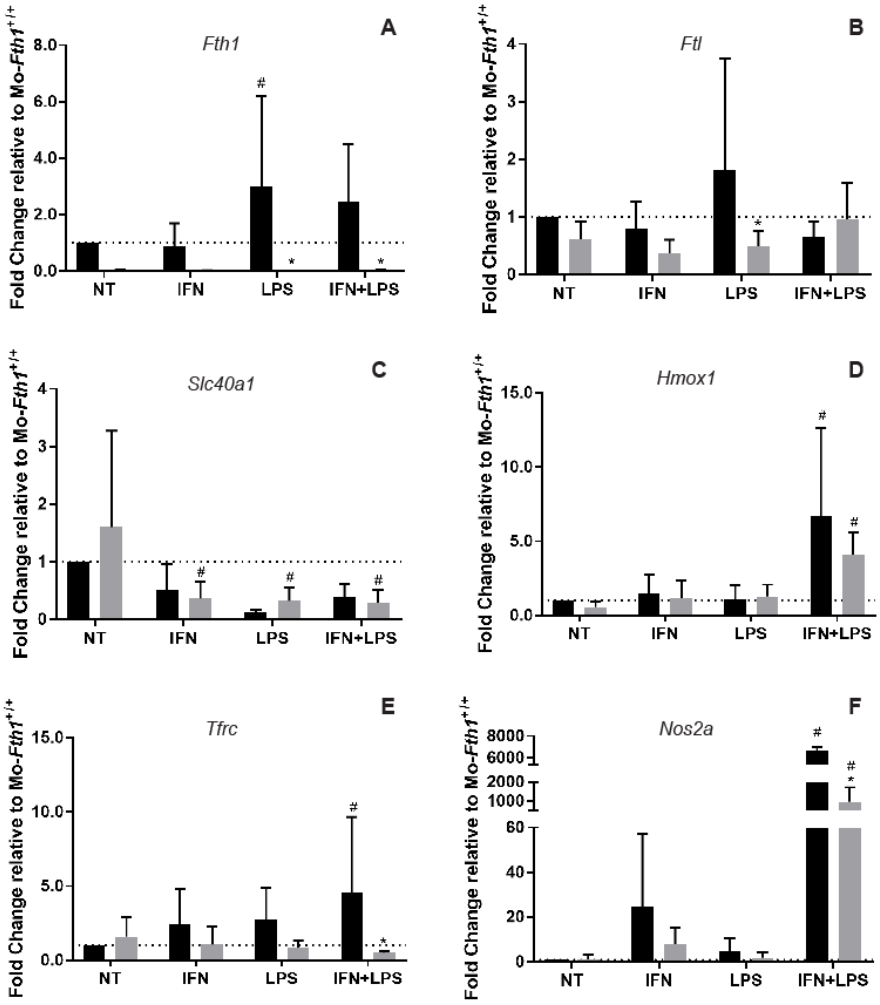

Figure 12 – **Iron metabolism genes have different expression responses to cytokines in Mo-*Fth1*$^{+/+}$ and Mo-*Fth1*$^{-/-}$.** After 7 days in culture, BMM were treated with IFN-γ, LPS or IFN-γ+LPS, and 3 days later the expression levels of several iron metabolism genes were quantified by qPCR. (**A**) H-ferritin (*Fth1*), (**B**) L-ferritin (*Ftl*), (**C**) ferroportin (*Slc40a1*), (**D**) heme oxygenase 1 (*Hmox1*), (**E**) transferrin receptor (*Tfrc*) and (**F**) inducible nitric oxide synthase (*Nos2a*). Data are expressed as mean + SD, presented as fold-change relatively to the non-treated (NT) Mo-*Fth1*$^{+/+}$ (n[Mo-*Fth1*$^{+/+}$] = 4; n[Mo-*Fth1*$^{-/-}$] = 7). Statistical analysis was performed using two-way ANOVA with Tukey's multiple comparisons. * $p < 0.05$ statistically significant between the two genotypes; # $p < 0.05$ statistically significant when comparing with the NT of Mo-*Fth1*$^{+/+}$.

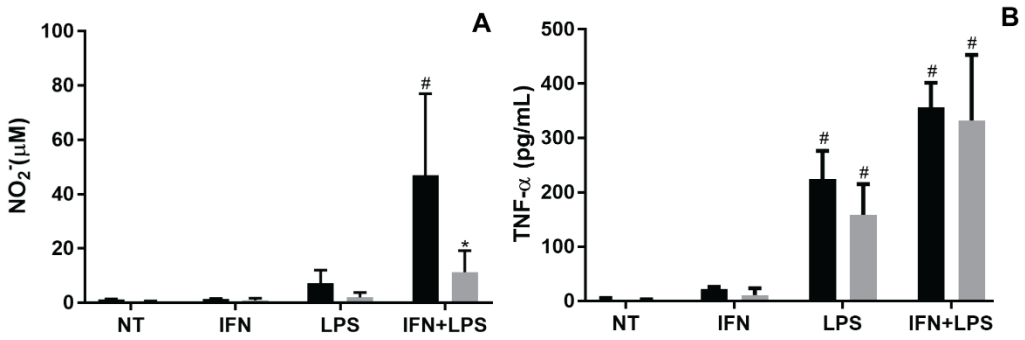

Figure 13 – Nitrite production is altered in Mo-*Fth1-/-*. Cells were treated with IFN-γ, LPS or IFN-γ+LPS, 7 days after the beginning of the cell culture. Nitrite production (**A**) and release of TNF-α (**B**) of Mo-*Fth1*$^{+/+}$ (black) and Mo-*Fth1*$^{-/-}$ (grey) was measured 3 days after cytokines treatment. **A**) Nitrite production was quantified by the Griess assay. **B**) TNF-α production was measured by ELISA. The graphs represent the mean + SD (n[Mo-*Fth1*$^{+/+}$] = 2; n[Mo-*Fth1*$^{-/-}$] = 6). Statistical analysis was performed using two-way ANOVA with Tukey's multiple comparisons test. * $p < 0.05$ when comparing the two genotypes. # $p < 0.05$ statistically significant when comparing with the corresponding NT sample.

Chapter 5

Discussion

The aim of this work was to study the impact of FTH1 in macrophages physiology. In order to accomplish that we made use of a mouse model with a conditional deletion of *Fth1* in the myeloid lineage (Darshan *et al.*, 2009).

Bearing this in mind, macrophages were obtained by differentiation from the BM of these mice and their viability, differentiation and morphology were characterized and compared with their littermates. Our data indicate that even though FTH1 is essential for the animal, as *Fth1* gene deficiency causes embryonic lethality (Ferreira *et al.*, 2000), Mo-*Fth1*$^{-/-}$ were similar to Mo-*Fth1*$^{+/+}$. This shows that under basal conditions (absence of stress or other stimulus), these macrophages can normally develop without H-ferritin (Fig. 4, 5 and 6).

In accordance, iron metabolism related genes, beyond *Fth1*, were not different between Mo-*Fth1*$^{+/+}$ and Mo-*Fth1*$^{-/-}$ (Fig. 8). Bolisetty *et al.* showed an increase in *Ftl* and *Hmox1* levels in macrophages isolated from injured kidneys of mice with a myeloid conditional deletion of *Fth1* (Bolisetty *et al.*, 2015). These distinct results can be explained by the culture conditions. In our work, macrophages were cultured in basal conditions, whereas in their work, macrophages were in a stimulated environment with a pro-inflammatory phenotype. Another interesting result was the one regarding genes related with iron transportation (*Tfrc* or *Slc40a1*). Vanoiaca *et al.* have demonstrated that in B cells with a *Fth1* conditional deletion, the LIP was significantly increased (Vanoaica *et al.*, 2014). As previously illustrated in figure 3, IRP/IRE controls the expression of several iron metabolism genes, depending on the intracellular iron levels. For instance, a higher LIP should decrease the binding affinity of IRP to IRE, inhibiting *Tfrc* and up-regulating *Slc40a1* (Wang and Pantopoulos, 2011). Nevertheless, in our work this was not observed, probably because LIP was not increased, as the cells were under basal conditions. In what concerns genes related with macrophage activation (*Nos2a, Arg1, Tnf*), no differences were found between both genotypes. On the other hand, it was reported a significant up-regulation in *Arg1* expression, again by Bolisetty *et al.*, in pro-inflammatory kidney macrophages (Bolisetty *et al.*, 2015). An important follow-up, would be to quantify the intracellular iron in both genotypes, which could be accomplished by using radioactive labeled-iron.

As previously discussed, Mo-*Fth1*$^{+/+}$ and Mo-*Fth1*$^{-/-}$ were similar and had no differences in their viability when in basal conditions. Thus, the next aim was to address if the same was true for exogenous iron-challenged cells. FAC and hemin caused a significant drop in the viability of both cell genotypes (Fig. 9A and B). This decrease in macrophage viability has been already

described for both FAC (Gan *et al.*, 2017) and hemin (Silva-Gomes *et al.*, 2013a). Interestingly, the lack of *Fth1* conferred a higher susceptibility to these compounds (Fig. 9A and B, Table 3). Cells that do not possess FTH1 are thought not to be able to handle iron as well as the ones who have the iron storage protein, leaving higher quantities of free-iron in the LIP. This free iron inside the cell (in our study, either from FAC or heme catabolized by HMOX1) can participate in the Waber-Weiss reaction leading to the formation of radicals that can cause damage to lipids, proteins, DNA and other intracellular organic molecules (Emerit *et al.*, 2001). These results correlate with Darshan *et al.*, as they showed that embryonic fibroblasts with a deletion of *Fth1* had more difficulty handling the exogenous iron (Darshan *et al.*, 2009). Even though both compounds were able to affect cell viability regardless of the genotype, the impact of FAC was stronger (Table 3). This may happen because FAC can passively enter the cell, whereas hemin needs a carrier (Khan and Quigley, 2011, Richardson and Baker, 1992). Theoretically, this suggests that, at the same concentrations, FAC will induce higher concentrations of free iron inside the cell, when comparing with hemin. Thus, this might explain the lower concentrations of FAC needed to reach 50% of cell viability (Table 3). To test this theory, it could be interesting to perform experiments with radioactive labeled-iron, as it was mentioned before.

In order to assess the toxicity mechanisms of these compounds, we evaluated their impact on cellular metabolism, permeability of plasmatic and nuclear membranes, and apoptosis. The results showed that the damage caused by FAC and hemin clearly promoted cell death (Fig. 9A, B and Fig. 10A, B). TUNEL assay showed that in Mo-*Fth1*$^{-/-}$, especially hemin, cell death is induced through apoptosis (Fig. 10D). Our findings correlate with data from Campos & Scorza showing that heme from oxidized RBC can induce apoptosis in J774A.1 MP cells (Cambos and Scorza, 2011). In the future, it would be interesting to understand how FAC and hemin are causing cell death. Thus, it would be important to assess if apoptosis inhibitors could revert the toxic effects of FAC and, especially hemin. Also, to evaluate if oxidative stress plays a role in the susceptibility of these cells, we could add an antioxidant, like N-acetylcysteine (NAC), to the iron treatments, or even address specific markers of this process (*e.g.* 8-OHdG).

On the other hand, with DFO, no differences were found in cell viability or cell death between the genotypes. Further, cell viability did not decrease below 50% even at the highest concentration tested (600 µM), not allowing to determine the IC_{50}. DFO is an iron chelator used in iron related diseases like hemochromatosis (Knovich *et al.*, 2009), because it binds iron, reducing its availability to the cells. This compound has low permeability, only entering the cell through endocytosis (De Domenico *et al.*, 2009b). This might explain the low toxicity observed even at the higher concentrations used (Fig. 9C). De Domenico *et al.* reported that DFO induces FTH1 degradation in lysosomes through autophagy (De Domenico *et al.*, 2009b). The similarity in both genotypes susceptibility may be explained by the degradation of FTH1 in the Mo-*Fth1*$^{+/+}$ to levels close to Mo-*Fth1*$^{-/-}$ phenotype. Moreover, the fact that the cellular viability did not decrease under 50%, combined with the absence of cell death with DFO (Fig.

10C and D), suggests, in line with the reports of De Domenico *et al.*, that cells may be using autophagy as a survival mechanism. Autophagy is an intracellular process used by cells as a quality control in order to remove protein aggregates, organelles and other strange components (Deretic *et al.*, 2013). This process is activated in stress conditions, hence it would be interesting to address if these cells are undergoing this process and what are the implications for their phenotype.

The latter part of this work, aimed to analyze the role of *Fth1* in macrophage activation. Therefore, both genotypes were challenged with well-known macrophage activators, as IFN-γ and LPS (Mosser and Zhang, 2008). IFN-γ has many functions in macrophages. It can stop macrophage growth and proliferation, and can activate these cells into a pro-inflammatory state, with induction of nitrites and reactive oxygen species. Also, it is known that LPS has a synergistic effect with IFN-γ on macrophage activation. LPS itself can activate macrophages via toll-like receptor 4 (TLR4), culminating in the production of pro-inflammatory cytokines like TNF-α (Schroder *et al.*, 2004).

Differently to iron treatments, only IFN-γ lowered cell viability and increased cell death of Mo-*Fth1*$^{-/-}$ (Fig. 11). IFN-γ and LPS are able to induce apoptosis due to the generation of nitrites (Seminara *et al.*, 2007), but that does not explain the higher death levels we observed in Mo-*Fth1*$^{-/-}$ treated with IFN-γ, because this was the treatment which caused the lower nitrite production (Fig. 13A). Moreover, Genin *et al.* reported an increased susceptibility of THP-1 monocytes to IFN-γ+LPS treatment when comparing to IFN-γ alone (Genin *et al.*, 2015). Sparse production of nitrites by IFN-γ treatment could be a consequence of the low concentrations given to the cells. Therefore, it should be interesting to increase IFN-γ doses and evaluate the nitrites production after. Additionally, as IFN-γ lowers cells' viability, even with a low production of nitrites, FTH1 may be playing a role in cellular protection, probably from oxidative stress. Future studies addressing the oxidative stress in Mo-*Fth1*$^{-/-}$ could be important, in order to understand the mechanisms by which this cytokine affects the cells.

Iron related genes expression was also evaluated, for each condition (Fig. 12). Regarding *Fth1*, only LPS induced its expression, in Mo-*Fth1*$^{+/+}$, which is in agreement of what been described by Mehlhase *et al.* in RAW264.7 murine macrophages (Mehlhase *et al.*, 2006). On the other hand, *Ftl* was not altered in any condition, suggesting that these treatments do not affect *Ftl* expression even, when *Fth1* was absent. In terms of iron transporters, *Slc40a1* was decreased in all treatments and genotypes, in accordance to what Agoro & Mura described about inflammation and macrophage activation (Agoro and Mura, 2016). Their findings suggest that *Slc40a1* is downregulated when macrophages are under a pro-inflammatory environment, which was the case of our experiments. Additionally, Van Zandt *et al.* reported differential regulation in *Slc40a1* expression during mycobacterial infection, depending on the type of macrophage (Van Zandt *et al.*, 2008). The data obtained for BMM correlate with our results, suggesting that,

being ferroportin the only known iron exporter, cells are accumulating iron under pro-inflammatory conditions. However, our results indicate that *Fth1* does not influence *Slc40a1* expression, as differences between genotypes were not obtained. Furthermore, *Tfrc* had a dual profile depending on the genotype. Indeed, in Mo-*Fth1*$^{+/+}$, *Tfrc* was increased, in line with the cellular need for iron referred above. Contrarily, in Mo-*Fth1*$^{-/-}$, the response was the opposite, suggesting that the lack of *Fth1* causes an alteration in iron metabolism dynamics. As the cell has lower iron storage capacity, it can neither export it, nor cope with the entry of more. Also, IFN-γ and LPS have been described in literature as inhibiting signals for *Tfrc* due to the induction of *Nos2a* and their effect on IRP2 (Kim and Ponka, 1999, 2000).

Regarding stress-inducible genes, our study was focused in *Hmox1* and *Nos2a*. The results show that only IFN-γ+LPS treatment induces an alteration in the expression of both genes in both genotypes (Fig. 12D and F). *Hmox1* is known to be increased in inflammatory environment, such as mycobacterial infection (Silva-Gomes *et al.*, 2013a), and in response to *Nos2a* levels (Ferreira *et al.*, 2009). In accordance, *Nos2a* was up-regulated in these conditions, in both genotypes. Increased *Nos2a* expression, induced by IFN-γ and LPS, is well described in the literature and is thought to be regulated by mitogen-activated protein kinase (MAPK) pathways (Chan and Riches, 2001). This gene was significantly more up-regulated in Mo-*Fth1*$^{+/+}$ than in Mo-*Fth1*$^{-/-}$ (Fig. 12F). FTH1 was shown to induce MAPK phosphorylation through a process involving PI3-kinase and nuclear factor kappa B (NF-kB) with subsequent *Nos2a* induction (Ruddell *et al.*, 2009). Nitrite production followed *Nos2a* expression, being highly increased in macrophages treated with IFN-γ+LPS and, as it happened in gene expression, Mo-*Fth1*$^{+/+}$ produced higher quantities of nitrites (Fig 13A).

Lastly, TNF-α was greatly increased in both genotypes, and in all treatments with LPS (Fig. 13B). Concordantly, LPS is known to induce TNF-α in macrophages. Actually, this effect has been well described in literature. LPS can induce TNF-α through stimulation of TLR4, by starting a signaling cascade in a MyD88 (myeloid differentiation primary response gene 88)-dependent pathway, activating NF-kB and MAPK (Lu *et al.*, 2008). No differences between the genotypes were found. IFN-γ synergized with LPS in TNF-α production, as Matic & Simon have shown in human monocyte-derived macrophages, correlating with our data (Matic and Simon, 1992).

Altogether, the data obtained within this work suggest that H-ferritin is an important player in iron metabolism dynamics in BMM, although it did not influence their viability, differentiation, and morphology in basal conditions. Despite that, Mo-*Fth1*$^{-/-}$ were more prone to iron metabolism deregulation when challenged by exogenous iron or by certain macrophage activators.

In the future, we intend to study the mechanisms beyond these effects and to further understand the role of FTH1 in macrophage physiology. To achieve that we will characterize the gene expression profile of Mo-*Fth1*$^{-/-}$ in response to exogenous iron. Moreover, it would be

interesting to compare the erythrophagocytosis process between the two genotypes. We have previously reported, H-ferritin as an important asset for mycobacteria survival in macrophages (Silva-Gomes *et al.*, 2013b). Thus, future experiments will be focused on a mycobacterial infection model of these macrophages lacking *Fth1* expression.

References

Agoro, R. and Mura, C. (2016). Inflammation-induced up-regulation of hepcidin and down-regulation of ferroportin transcription are dependent on macrophage polarization. *Blood Cells Mol Dis*, 61, 16-25. 10.1016/j.bcmd.2016.07.006

Aisen, P., Leibman, A. and Zweier, J. (1978). Stoichiometric and site characteristics of the binding of iron to human transferrin. *J Biol Chem*, 253, 1930-7.

Allen, L. H. (2000). Anemia and iron deficiency: effects on pregnancy outcome. *Am J Clin Nutr*, 71, 1280S-4S.

Alleyne, M., Horne, M. K. and Miller, J. L. (2008). Individualized treatment for iron-deficiency anemia in adults. *Am J Med*, 121, 943-8. 10.1016/j.amjmed.2008.07.012

Arosio, P., Carmona, F., Gozzelino, R., Maccarinelli, F. and Poli, M. (2015). The importance of eukaryotic ferritins in iron handling and cytoprotection. *Biochem J*, 472, 1-15. 10.1042/BJ20150787

Austyn, J. M. and Gordon, S. (1981). F4/80, a monoclonal antibody directed specifically against the mouse macrophage. *Eur J Immunol*, 11, 805-15. 10.1002/eji.1830111013

Bolisetty, S., Zarjou, A., Hull, T. D., Traylor, A. M., Perianayagam, A., Joseph, R., Kamal, A. I., Arosio, P., Soares, M. P., Jeney, V., Balla, J., George, J. F. and Agarwal, A. (2015). Macrophage and epithelial cell H-ferritin expression regulates renal inflammation. *Kidney Int*, 88, 95-108. 10.1038/ki.2015.102

Bratosin, D., Mazurier, J., Tissier, J. P., Estaquier, J., Huart, J. J., Ameisen, J. C., Aminoff, D. and Montreuil, J. (1998). Cellular and molecular mechanisms of senescent erythrocyte phagocytosis by macrophages. A review. *Biochimie*, 80, 173-95.

Cambos, M. and Scorza, T. (2011). Robust erythrophagocytosis leads to macrophage apoptosis via a hemin-mediated redox imbalance: role in hemolytic disorders. *J Leukoc Biol*, 89, 159-71. 10.1189/jlb.0510249

Carmona, U., Li, L., Zhang, L. and Knez, M. (2014). Ferritin light-chain subunits: key elements for the electron transfer across the protein cage. *Chem Commun (Camb)*, 50, 15358-61. 10.1039/c4cc07996e

Cassat, J. E. and Skaar, E. P. (2013). Iron in infection and immunity. *Cell Host Microbe*, 13, 509-19. 10.1016/j.chom.2013.04.010

Chan, E. D. and Riches, D. W. (2001). IFN-gamma + LPS induction of iNOS is modulated by ERK, JNK/SAPK, and p38(mapk) in a mouse macrophage cell line. *Am J Physiol Cell Physiol*, 280, C441-50.

Chasteen, N. D. and Harrison, P. M. (1999). Mineralization in ferritin: an efficient means of iron storage. *J Struct Biol*, 126, 182-94. 10.1006/jsbi.1999.4118

Chen, T. T., Li, L., Chung, D. H., Allen, C. D., Torti, S. V., Torti, F. M., Cyster, J. G., Chen, C. Y., Brodsky, F. M., Niemi, E. C., Nakamura, M. C., Seaman, W. E. and Daws, M. R. (2005). TIM-2 is expressed on B cells and in liver and kidney and is a receptor for H-ferritin endocytosis. *J Exp Med*, 202, 955-65. 10.1084/jem.20042433

Cherukuri, S., Potla, R., Sarkar, J., Nurko, S., Harris, Z. L. and Fox, P. L. (2005). Unexpected role of ceruloplasmin in intestinal iron absorption. *Cell Metab*, 2, 309-19. 10.1016/j.cmet.2005.10.003

Chow, A., Huggins, M., Ahmed, J., Hashimoto, D., Lucas, D., Kunisaki, Y., Pinho, S., Leboeuf, M., Noizat, C., van Rooijen, N., Tanaka, M., Zhao, Z. J., Bergman, A., Merad, M. and Frenette, P. S. (2013). CD169(+) macrophages provide a niche promoting erythropoiesis under homeostasis and stress. *Nat Med*, 19, 429-36. 10.1038/nm.3057

Cohen, L. A., Gutierrez, L., Weiss, A., Leichtmann-Bardoogo, Y., Zhang, D. L., Crooks, D. R., Sougrat, R., Morgenstern, A., Galy, B., Hentze, M. W., Lazaro, F. J., Rouault, T. A. and Meyron-Holtz, E. G. (2010). Serum ferritin is derived primarily from macrophages through a nonclassical secretory pathway. *Blood*, 116, 1574-84. 10.1182/blood-2009-11-253815

Cumano, A. and Godin, I. (2007). Ontogeny of the hematopoietic system. *Annu Rev Immunol*, 25, 745-85. 10.1146/annurev.immunol.25.022106.141538

D'Angelo, G. (2013). Role of hepcidin in the pathophysiology and diagnosis of anemia. *Blood Res*, 48, 10-5. 10.5045/br.2013.48.1.10

Daniels, T. R., Delgado, T., Rodriguez, J. A., Helguera, G. and Penichet, M. L. (2006). The transferrin receptor part I: Biology and targeting with cytotoxic antibodies for the treatment of cancer. *Clin Immunol*, 121, 144-58. 10.1016/j.clim.2006.06.010

Darshan, D., Vanoaica, L., Richman, L., Beermann, F. and Kuhn, L. C. (2009). Conditional deletion of ferritin H in mice induces loss of iron storage and liver damage. *Hepatology*, 50, 852-60. 10.1002/hep.23058

Davies, L. C., Jenkins, S. J., Allen, J. E. and Taylor, P. R. (2013). Tissue-resident macrophages. *Nat Immunol*, 14, 986-95. 10.1038/ni.2705

de Back, D. Z., Kostova, E. B., van Kraaij, M., van den Berg, T. K. and van Bruggen, R. (2014). Of macrophages and red blood cells; a complex love story. *Front Physiol*, 5, 9. 10.3389/fphys.2014.00009

De Domenico, I., Lo, E., Ward, D. M. and Kaplan, J. (2009a). Hepcidin-induced internalization of ferroportin requires binding and cooperative interaction with Jak2. *Proc Natl Acad Sci U S A*, 106, 3800-5. 10.1073/pnas.0900453106

De Domenico, I., Ward, D. M. and Kaplan, J. (2009b). Specific iron chelators determine the route of ferritin degradation. *Blood*, 114, 4546-51. 10.1182/blood-2009-05-224188

Delaby, C., Pilard, N., Goncalves, A. S., Beaumont, C. and Canonne-Hergaux, F. (2005). Presence of the iron exporter ferroportin at the plasma membrane of macrophages is enhanced by iron loading and down-regulated by hepcidin. *Blood*, 106, 3979-84. 10.1182/blood-2005-06-2398

Deretic, V., Saitoh, T. and Akira, S. (2013). Autophagy in infection, inflammation and immunity. *Nat Rev Immunol*, 13, 722-37. 10.1038/nri3532

Donovan, A., Lima, C. A., Pinkus, J. L., Pinkus, G. S., Zon, L. I., Robine, S. and Andrews, N. C. (2005). The iron exporter ferroportin/Slc40a1 is essential for iron homeostasis. *Cell Metab*, 1, 191-200. 10.1016/j.cmet.2005.01.003

Eaton, J. W. and Qian, M. (2002). Molecular bases of cellular iron toxicity. *Free Radic Biol Med*, 32, 833-40.

Emerit, J., Beaumont, C. and Trivin, F. (2001). Iron metabolism, free radicals, and oxidative injury. *Biomed Pharmacother*, 55, 333-9.

Evstatiev, R. and Gasche, C. (2012). Iron sensing and signalling. *Gut*, 61, 933-52. 10.1136/gut.2010.214312

Ferreira, A. M., Ferrari, M. I., Trostchansky, A., Batthyany, C., Souza, J. M., Alvarez, M. N., Lopez, G. V., Baker, P. R., Schopfer, F. J., O'Donnell, V., Freeman, B. A. and Rubbo, H. (2009). Macrophage activation induces formation of the anti-inflammatory lipid cholesteryl-nitrolinoleate. *Biochem J*, 417, 223-34. 10.1042/BJ20080701

Ferreira, C., Bucchini, D., Martin, M. E., Levi, S., Arosio, P., Grandchamp, B. and Beaumont, C. (2000). Early embryonic lethality of H ferritin gene deletion in mice. *J Biol Chem*, 275, 3021-4.

Gan, Z. S., Wang, Q. Q., Li, J. H., Wang, X. L., Wang, Y. Z. and Du, H. H. (2017). Iron Reduces M1 Macrophage Polarization in RAW264.7 Macrophages Associated with Inhibition of STAT1. *Mediators Inflamm*, 2017, 8570818. 10.1155/2017/8570818

Geissmann, F., Manz, M. G., Jung, S., Sieweke, M. H., Merad, M. and Ley, K. (2010). Development of monocytes, macrophages, and dendritic cells. *Science*, 327, 656-61. 10.1126/science.1178331

Genin, M., Clement, F., Fattaccioli, A., Raes, M. and Michiels, C. (2015). M1 and M2 macrophages derived from THP-1 cells differentially modulate the response of cancer cells to etoposide. *BMC Cancer*, 15, 577. 10.1186/s12885-015-1546-9

Getz, G. S. (2005). Thematic review series: the immune system and atherogenesis. Bridging the innate and adaptive immune systems. *J Lipid Res*, 46, 619-22. 10.1194/jlr.E500002-JLR200

Ghosh, S., Hevi, S. and Chuck, S. L. (2004). Regulated secretion of glycosylated human ferritin from hepatocytes. *Blood*, 103, 2369-76. 10.1182/blood-2003-09-3050

Jauregui-Lobera, I. (2014). Iron deficiency and cognitive functions. *Neuropsychiatr Dis Treat*, 10, 2087-95. 10.2147/NDT.S72491

Kakhlon, O. and Cabantchik, Z. I. (2002). The labile iron pool: characterization, measurement, and participation in cellular processes(1). *Free Radic Biol Med*, 33, 1037-46.

Khan, A. A. and Quigley, J. G. (2011). Control of intracellular heme levels: heme transporters and heme oxygenases. *Biochim Biophys Acta*, 1813, 668-82. 10.1016/j.bbamcr.2011.01.008

Kim, S. and Ponka, P. (1999). Control of transferrin receptor expression via nitric oxide-mediated modulation of iron-regulatory protein 2. *J Biol Chem*, 274, 33035-42.

Kim, S. and Ponka, P. (2000). Effects of interferon-gamma and lipopolysaccharide on macrophage iron metabolism are mediated by nitric oxide-induced degradation of iron regulatory protein 2. *J Biol Chem*, 275, 6220-6.

Knovich, M. A., Storey, J. A., Coffman, L. G., Torti, S. V. and Torti, F. M. (2009). Ferritin for the clinician. *Blood Rev*, 23, 95-104. 10.1016/j.blre.2008.08.001

Kondo, H., Saito, K., Grasso, J. P. and Aisen, P. (1988). Iron metabolism in the erythrophagocytosing Kupffer cell. *Hepatology*, 8, 32-8.

Kurotaki, D., Uede, T. and Tamura, T. (2015). Functions and development of red pulp macrophages. *Microbiol Immunol*, 59, 55-62. 10.1111/1348-0421.12228

Latunde-Dada, G. O., Simpson, R. J. and McKie, A. T. (2008). Duodenal cytochrome B expression stimulates iron uptake by human intestinal epithelial cells. *J Nutr*, 138, 991-5.

Lawson, D. M., Artymiuk, P. J., Yewdall, S. J., Smith, J. M., Livingstone, J. C., Treffry, A., Luzzago, A., Levi, S., Arosio, P., Cesareni, G. and et al. (1991). Solving the structure of human H ferritin by genetically engineering intermolecular crystal contacts. *Nature*, 349, 541-4. 10.1038/349541a0

Leimberg, M. J., Prus, E., Konijn, A. M. and Fibach, E. (2008). Macrophages function as a ferritin iron source for cultured human erythroid precursors. *J Cell Biochem*, 103, 1211-8. 10.1002/jcb.21499

Levi, S., Corsi, B., Bosisio, M., Invernizzi, R., Volz, A., Sanford, D., Arosio, P. and Drysdale, J. (2001). A human mitochondrial ferritin encoded by an intronless gene. *J Biol Chem*, 276, 24437-40. 10.1074/jbc.C100141200

Li, J. Y., Paragas, N., Ned, R. M., Qiu, A., Viltard, M., Leete, T., Drexler, I. R., Chen, X., Sanna-Cherchi, S., Mohammed, F., Williams, D., Lin, C. S., Schmidt-Ott, K. M., Andrews, N. C. and Barasch, J. (2009). Scara5 is a ferritin receptor mediating non-transferrin iron delivery. *Dev Cell*, 16, 35-46. 10.1016/j.devcel.2008.12.002

Li, L., Fang, C. J., Ryan, J. C., Niemi, E. C., Lebron, J. A., Bjorkman, P. J., Arase, H., Torti, F. M., Torti, S. V., Nakamura, M. C. and Seaman, W. E. (2010). Binding and uptake of H-ferritin are mediated by human transferrin receptor-1. *Proc Natl Acad Sci U S A*, 107, 3505-10. 10.1073/pnas.0913192107

Lieu, P. T., Heiskala, M., Peterson, P. A. and Yang, Y. (2001). The roles of iron in health and disease. *Mol Aspects Med*, 22, 1-87.

Lin, L., Valore, E. V., Nemeth, E., Goodnough, J. B., Gabayan, V. and Ganz, T. (2007). Iron transferrin regulates hepcidin synthesis in primary hepatocyte culture through hemojuvelin and BMP2/4. *Blood*, 110, 2182-9. 10.1182/blood-2007-04-087593

Liu, Q., Davidoff, O., Niss, K. and Haase, V. H. (2012). Hypoxia-inducible factor regulates hepcidin via erythropoietin-induced erythropoiesis. *J Clin Invest*, 122, 4635-44. 10.1172/JCI63924

Lu, Y. C., Yeh, W. C. and Ohashi, P. S. (2008). LPS/TLR4 signal transduction pathway. *Cytokine*, 42, 145-51. 10.1016/j.cyto.2008.01.006

Luscieti, S., Santambrogio, P., Langlois d'Estaintot, B., Granier, T., Cozzi, A., Poli, M., Gallois, B., Finazzi, D., Cattaneo, A., Levi, S. and Arosio, P. (2010). Mutant ferritin L-chains that cause

neurodegeneration act in a dominant-negative manner to reduce ferritin iron incorporation. *J Biol Chem*, 285, 11948-57. 10.1074/jbc.M109.096404

Matic, M. and Simon, S. R. (1992). Effects of gamma interferon on release of tumor necrosis factor alpha from lipopolysaccharide-tolerant human monocyte-derived macrophages. *Infect Immun*, 60, 3756-62.

Mehlhase, J., Gieche, J., Widmer, R. and Grune, T. (2006). Ferritin levels in microglia depend upon activation: modulation by reactive oxygen species. *Biochim Biophys Acta*, 1763, 854-9. 10.1016/j.bbamcr.2006.04.012

Miller, J. L. (2013). Iron deficiency anemia: a common and curable disease. *Cold Spring Harb Perspect Med*, 3. 10.1101/cshperspect.a011866

Mosser, D. M. and Zhang, X. (2008). Activation of murine macrophages. *Curr Protoc Immunol*, Chapter 14, Unit 14 2. 10.1002/0471142735.im1402s83

Muckenthaler, M. U., Galy, B. and Hentze, M. W. (2008). Systemic iron homeostasis and the iron-responsive element/iron-regulatory protein (IRE/IRP) regulatory network. *Annu Rev Nutr*, 28, 197-213. 10.1146/annurev.nutr.28.061807.155521

Nairz, M., Schroll, A., Demetz, E., Tancevski, I., Theurl, I. and Weiss, G. (2015). 'Ride on the ferrous wheel'--the cycle of iron in macrophages in health and disease. *Immunobiology*, 220, 280-94. 10.1016/j.imbio.2014.09.010

Nemeth, E., Tuttle, M. S., Powelson, J., Vaughn, M. B., Donovan, A., Ward, D. M., Ganz, T. and Kaplan, J. (2004). Hepcidin regulates cellular iron efflux by binding to ferroportin and inducing its internalization. *Science*, 306, 2090-3. 10.1126/science.1104742

Nicolas, G., Chauvet, C., Viatte, L., Danan, J. L., Bigard, X., Devaux, I., Beaumont, C., Kahn, A. and Vaulont, S. (2002). The gene encoding the iron regulatory peptide hepcidin is regulated by anemia, hypoxia, and inflammation. *J Clin Invest*, 110, 1037-44. 10.1172/JCI15686

Ohgami, R. S., Campagna, D. R., Greer, E. L., Antiochos, B., McDonald, A., Chen, J., Sharp, J. J., Fujiwara, Y., Barker, J. E. and Fleming, M. D. (2005). Identification of a ferrireductase required for efficient transferrin-dependent iron uptake in erythroid cells. *Nat Genet*, 37, 1264-9. 10.1038/ng1658

Parrow, N. L., Fleming, R. E. and Minnick, M. F. (2013). Sequestration and scavenging of iron in infection. *Infect Immun*, 81, 3503-14. 10.1128/IAI.00602-13

Podolnikova, N. P., Kushchayeva, Y. S., Wu, Y., Faust, J. and Ugarova, T. P. (2016). The Role of Integrins alphaMbeta2 (Mac-1, CD11b/CD18) and alphaDbeta2 (CD11d/CD18) in Macrophage Fusion. *Am J Pathol*, 186, 2105-2116. 10.1016/j.ajpath.2016.04.001

Recalcati, S., Invernizzi, P., Arosio, P. and Cairo, G. (2008). New functions for an iron storage protein: the role of ferritin in immunity and autoimmunity. *J Autoimmun*, 30, 84-9. 10.1016/j.jaut.2007.11.003

Richardson, D. and Baker, E. (1992). Two mechanisms of iron uptake from transferrin by melanoma cells. The effect of desferrioxamine and ferric ammonium citrate. *J Biol Chem*, 267, 13972-9.

Ruddell, R. G., Hoang-Le, D., Barwood, J. M., Rutherford, P. S., Piva, T. J., Watters, D. J., Santambrogio, P., Arosio, P. and Ramm, G. A. (2009). Ferritin functions as a proinflammatory cytokine via iron-independent protein kinase C zeta/nuclear factor kappaB-regulated signaling in rat hepatic stellate cells. *Hepatology*, 49, 887-900. 10.1002/hep.22716

Schroder, K., Hertzog, P. J., Ravasi, T. and Hume, D. A. (2004). Interferon-gamma: an overview of signals, mechanisms and functions. *J Leukoc Biol*, 75, 163-89. 10.1189/jlb.0603252

Seminara, A. R., Ruvolo, P. P. and Murad, F. (2007). LPS/IFNgamma-induced RAW 264.7 apoptosis is regulated by both nitric oxide-dependent and -independent pathways involving JNK and the Bcl-2 family. *Cell Cycle*, 6, 1772-8. 10.4161/cc.6.14.4438

Silva-Gomes, S., Appelberg, R., Larsen, R., Soares, M. P. and Gomes, M. S. (2013a). Heme catabolism by heme oxygenase-1 confers host resistance to Mycobacterium infection. *Infect Immun*, 81, 2536-45. 10.1128/IAI.00251-13

Silva-Gomes, S., Bouton, C., Silva, T., Santambrogio, P., Rodrigues, P., Appelberg, R. and Gomes, M. S. (2013b). Mycobacterium avium infection induces H-ferritin expression in mouse primary macrophages by activating Toll-like receptor 2. *PLoS One*, 8, e82874. 10.1371/journal.pone.0082874

Smith, A. and McCulloh, R. J. (2015). Hemopexin and haptoglobin: allies against heme toxicity from hemoglobin not contenders. *Front Physiol*, 6, 187. 10.3389/fphys.2015.00187

Soares, M. P. and Hamza, I. (2016). Macrophages and Iron Metabolism. *Immunity*, 44, 492-504. 10.1016/j.immuni.2016.02.016

Tenhunen, R., Marver, H. S. and Schmid, R. (1968). The enzymatic conversion of heme to bilirubin by microsomal heme oxygenase. *Proc Natl Acad Sci U S A*, 61, 748-55.

Theil, E. C. (1987). Ferritin: structure, gene regulation, and cellular function in animals, plants, and microorganisms. *Annu Rev Biochem*, 56, 289-315. 10.1146/annurev.bi.56.070187.001445

Thompson, K. J., Fried, M. G., Ye, Z., Boyer, P. and Connor, J. R. (2002). Regulation, mechanisms and proposed function of ferritin translocation to cell nuclei. *J Cell Sci*, 115, 2165-77.

Torti, F. M. and Torti, S. V. (2002). Regulation of ferritin genes and protein. *Blood*, 99, 3505-16.

Trinder, D., Zak, O. and Aisen, P. (1996). Transferrin receptor-independent uptake of differic transferrin by human hepatoma cells with antisense inhibition of receptor expression. *Hepatology*, 23, 1512-20. 10.1053/jhep.1996.v23.pm0008675172

Van Zandt, K. E., Sow, F. B., Florence, W. C., Zwilling, B. S., Satoskar, A. R., Schlesinger, L. S. and Lafuse, W. P. (2008). The iron export protein ferroportin 1 is differentially expressed in mouse macrophage populations and is present in the mycobacterial-containing phagosome. *J Leukoc Biol*, 84, 689-700. 10.1189/jlb.1107781

Vanoaica, L., Richman, L., Jaworski, M., Darshan, D., Luther, S. A. and Kuhn, L. C. (2014). Conditional deletion of ferritin h in mice reduces B and T lymphocyte populations. *PLoS One*, 9, e89270. 10.1371/journal.pone.0089270

Varol, C., Mildner, A. and Jung, S. (2015). Macrophages: development and tissue specialization. *Annu Rev Immunol*, 33, 643-75. 10.1146/annurev-immunol-032414-112220

Vulpe, C. D., Kuo, Y. M., Murphy, T. L., Cowley, L., Askwith, C., Libina, N., Gitschier, J. and Anderson, G. J. (1999). Hephaestin, a ceruloplasmin homologue implicated in intestinal iron transport, is defective in the sla mouse. *Nat Genet*, 21, 195-9. 10.1038/5979

Wang, C. Y. and Babitt, J. L. (2016). Hepcidin regulation in the anemia of inflammation. *Curr Opin Hematol*, 23, 189-97. 10.1097/MOH.0000000000000236

Wang, J. and Pantopoulos, K. (2011). Regulation of cellular iron metabolism. *Biochem J*, 434, 365-81. 10.1042/BJ20101825

Wang, W., Knovich, M. A., Coffman, L. G., Torti, F. M. and Torti, S. V. (2010). Serum ferritin: Past, present and future. *Biochim Biophys Acta*, 1800, 760-9. 10.1016/j.bbagen.2010.03.011

Weinberg, E. D. (2009). Iron toxicity: new conditions continue to emerge. *Oxid Med Cell Longev*, 2, 107-9.

Wilkinson, N. and Pantopoulos, K. (2014). The IRP/IRE system in vivo: insights from mouse models. *Front Pharmacol*, 5, 176. 10.3389/fphar.2014.00176

Winterbourn, C. C. (1995). Toxicity of iron and hydrogen peroxide: the Fenton reaction. *Toxicol Lett*, 82-83, 969-74.

Worwood, M., Brook, J. D., Cragg, S. J., Hellkuhl, B., Jones, B. M., Perera, P., Roberts, S. H. and Shaw, D. J. (1985). Assignment of human ferritin genes to chromosomes 11 and 19q13.3---19qter. *Hum Genet*, 69, 371-4.

Zhao, N., Zhang, A. S. and Enns, C. A. (2013). Iron regulation by hepcidin. *J Clin Invest*, 123, 2337-43. 10.1172/JCI67225

Zigmond, E. and Jung, S. (2013). Intestinal macrophages: well educated exceptions from the rule. *Trends Immunol*, 34, 162-8. 10.1016/j.it.2013.02.001